

UBV CCD PHOTOMETRY OF THE INTERMEDIATE AGE OPEN CLUSTER NGC 6716

CHUN, Moo-YOUNG

Bohyunsan Optical Astronomy Observatory, Korea Astronomy Observatory,
Youngchun, Kyungbook 770-820, Korea
Electronic mail: mychun@seeru.boao.re.kr

AND

LEE, SEE-WOO

Department of Astronomy, Seoul National University, Seoul 151-742, Korea
Electronic mail: swlee@astropop.snu.ac.kr

(Received September 23, 1996; Accepted October 14, 1996)

ABSTRACT

NGC 6716 is an intermediate-age open cluster in Sagittarius. In this paper, we present the new UBV CCD photometry of the stars in the cluster, which is deeper than previous ones. From the color-color diagram and the color-magnitude diagram, we derived a reddening $E_{B-V} = 0.17 \pm 0.03$ and a distance modulus of the cluster, $(V - M_V)_o = 9.2 \pm 0.1$. An age of the cluster is estimated as 8×10^7 yrs from the latest isochrone. Luminosity function and mass function of the cluster are derived. The gradient of the mass function of bright stars is a bit steep, $\Gamma = -1.85 \pm 0.05$, and there is no distinct bump and dip in the mass function.

Key Words : clusters: open — individual: NGC 6716, photometry, luminosity function, mass function

I. INTRODUCTION

NGC 6716($\alpha_{1950}=18^h\ 51.^m6$, $\delta_{1950}=-19^\circ\ 58'$; $l=15^\circ.4$, $b=-9^\circ.6$) is a small open cluster in Sagittarius, situated far away from the galactic plane. Trumpler(1930) classified the cluster as class II 3p, but Ruprecht(1966) classified the cluster as class IV 1p, which seems to be more reasonable than the previous one.

Lindoff(1971: hereafter LD) established 12 photoelectric standards in the range $V = 8.28 \sim 13.29$ in the cluster field as a calibration sequence for UBV photographic photometry of 115 stars down to $V = 13.79$. Turner & Pedreros(1985) investigated this cluster and another open cluster Cr 394, which is 40' far from the former, and concluded that they form a double cluster since they lie at similar distances and have close similarity in ages. They have done UBVRI_{KC} photoelectric photometry of only 13 bright stars in the cluster field. Grice & Dawson(1990; hereafter GD) have extended the LD's work increasing the number of photoelectric standards to 24 stars and also have done the photographic photometry down to $V=16.0$.

In Section 2, we present the observations and the data reduction. Section 3 describes the features of the resulting CMD, color excess, distance modulus, and age of the cluster. Section 4 is devoted to deriving luminosity function and mass function of the cluster, and brief discussion and summary of the present study are given in Section 5.

II. OBSERVATIONS AND DATA REDUCTION

(a) Observations

The observations have been performed using the Siding Spring Observatory(SSO) 40 inch telescope equipped with a CCD camera at the F/8 focus in August 1993. The CCD camera used, so called TCCD, was a Tektronics

NGC 6716

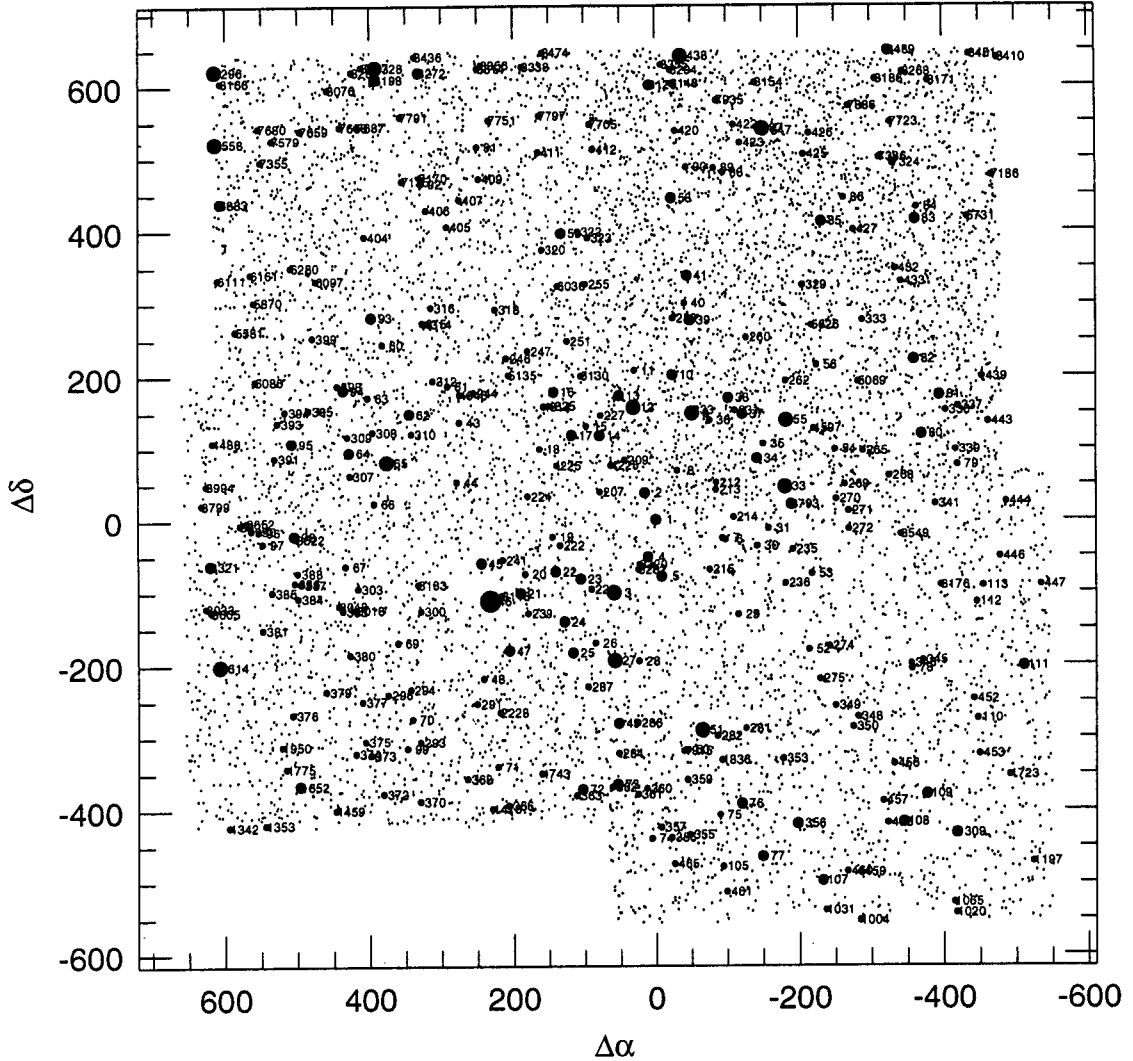


Fig. 1. Identification Chart of observed NGC 6716 field. No. 1 star is centered on this field. North is up and East is left. The scale is in unit of arcsec. IDs less than 1000 is attributed to Lindoff (1971) and Grice & Dawson (1990).

AR-coated 1024×1024 pixels array. The sky area covered by a single frame is about $10' \times 10'$. We chose a lower gain ($1e^-/\text{ADU}$) between two selectable gains. The characteristics of UBV filters are very similar to those of Johnson-Cousins standard filters (Bessell 1990).

As the apparent size of NGC 6716 is larger than the field of view by the single frame of TCCD, we divided the cluster into 4 subregions - NW, NE, SW, and SE. More than 3 sets of UBV CCD images for each region were obtained with overlapping regions of about 1 arcmin. We assigned the bright stars as the same IDs with LD & GD. Since the observations are deeper than LD's & GD's, we assigned the faint stars, which are not identified by LD & GD, as new IDs of the sequential numbers larger than 1000 in order of their declination. Fig. 1 is a finding chart of the cluster. The stars brighter than $V = 15^m$ are shown with IDs.

(b) Data Reduction and Accuracy of Observation

The CCD frames were preprocessed by subtracting the bias level determined from the overscan regions, dividing by twilight sky flats, and trimming the overscan regions and unreliable regions. All procedures were performed with the IRAF/CCDRED package running on a SUN Sparcstation. Photometry of the stars was carried out for each frame

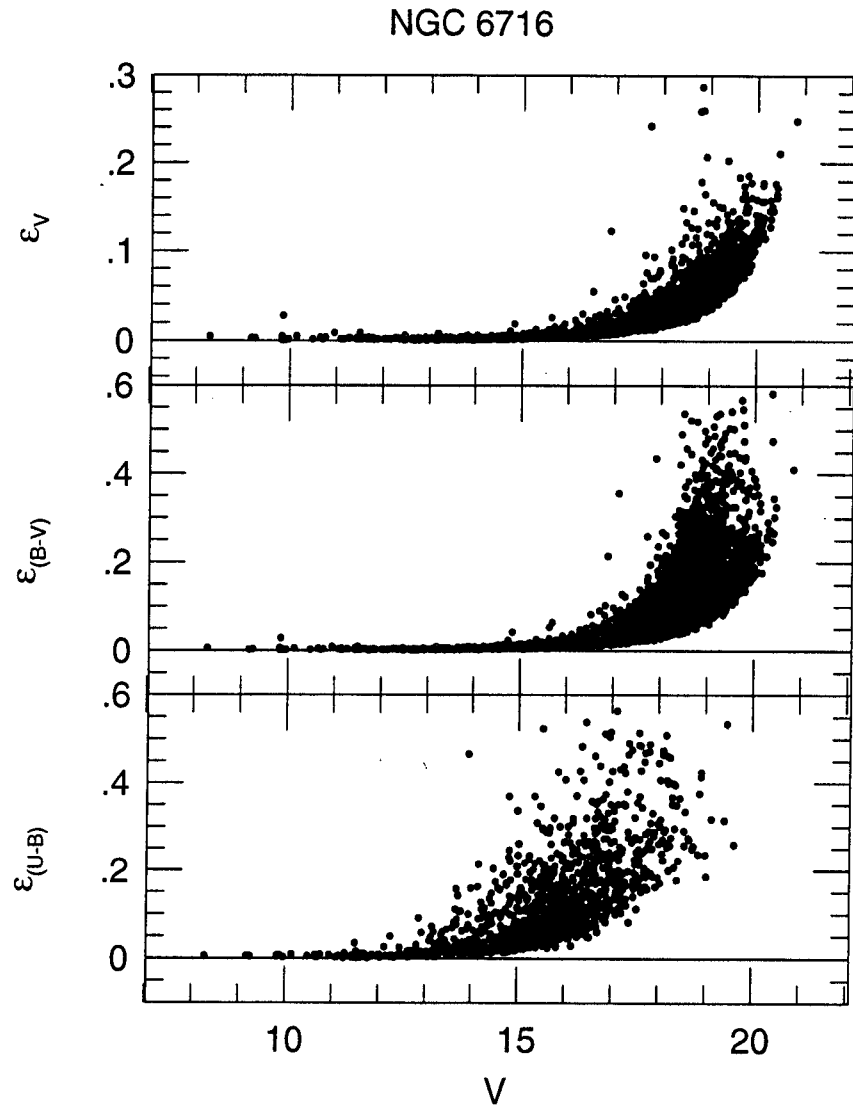


Fig. 2. Relation between photometric errors estimated from DAOPHOT and standard V magnitude.

with the IRAF version of DAOPHOT (Stetson 1987, 1991) using PSF fitting method for cluster and simple aperture photometry for standard stars.

The transformation equations from the instrumental magnitudes (v, b, u) to the standard system (V, B, U) are as follows:

$$\begin{aligned} v &= V + \text{zero}_v + (-0.039 \pm 0.011)(B - V) \\ b &= B + \text{zero}_b + (-0.065 \pm 0.013)(B - V) \\ u &= U + \text{zero}_u + (-0.136 \pm 0.029)(U - B), \end{aligned} \quad (1)$$

where we used standard stars in equatorial standard fields (Landolt 1992) and NGC 300 standard field (Graham 1981) observed during this observing period. The zero points were determined by common stars with the photoelectric data of GD. As there were few photoelectric stars in NE & SE regions, we adjusted the zero points of those regions with accuracies less than 0.05 mag, using CCD photometric data of the stars in the overlapped regions.

The mean values of magnitude and colors of stars which are observed many times were determined weighting by

Table 1. Photometric Data in NGC 6716

ID	$\Delta\alpha''$	$\Delta\delta''$	V	ϵ_V	B-V	ϵ_{B-V}	U-B	ϵ_{U-B}	ID	$\Delta\alpha''$	$\Delta\delta''$	V	ϵ_V	B-V	ϵ_{B-V}	U-B	ϵ_{U-B}
1	0.0	0.0	12.957	0.002	1.091	0.004	0.763	0.009	75	-89.4	-407.3	13.078	0.002	0.668	0.003	0.128	0.005
2	15.3	37.1	11.716	0.002	0.256	0.002	0.219	0.010	76	-119.9	-392.0	12.908	0.004	1.372	0.006	1.479	0.016
3	59.3	-101.0	9.170	0.003	0.024	0.003	-0.360	0.006	77	-148.9	-464.5	12.654	0.001	0.648	0.002	0.147	0.004
4	11.2	-51.7	11.088	0.002	0.185	0.004	0.028	0.003	78	-355.6	-206.2	13.524	0.003	0.582	0.004	0.007	0.007
5	-7.7	-78.5	12.044	0.002	0.332	0.003	0.107	0.003	79	-419.3	75.8	13.641	0.003	1.752	0.005	1.937	0.082
6	-97.7	-27.9	13.285	0.003	1.675	0.006			80	-369.9	119.1	12.913	0.002	0.659	0.003	0.208	0.006
7	-93.4	-25.8	13.910	0.003	0.690	0.005	0.085	0.013	81	-394.5	173.0	12.702	0.002	1.386	0.003	1.637	0.018
8	-30.1	68.1	13.946	0.003	1.662	0.005	2.247	0.100	82	-359.2	222.1	12.629	0.003	1.394	0.004	1.605	0.017
9	-51.3	148.5	10.677	0.003	0.230	0.004	0.033	0.003	83	-361.1	414.5	11.606	0.003	0.239	0.004	0.131	0.003
10	-23.8	200.9	12.016	0.002	1.070	0.003	0.886	0.009	84	-363.4	431.5	13.747	0.004	1.289	0.006	1.181	0.018
11	29.9	207.4	13.708	0.002	0.622	0.003	0.116	0.016	85	-231.0	411.6	11.434	0.003	0.484	0.004	0.200	0.003
12	31.1	156.5	9.967	0.002	0.068	0.003	-0.044	0.003	86	-262.1	444.0	13.364	0.004	1.375	0.006	1.468	0.024
13	51.5	172.9	12.485	0.002	0.399	0.002	0.233	0.009	87	-149.6	539.5	10.144	0.005	0.695	0.006	0.263	0.009
14	78.3	117.8	11.150	0.002	0.123	0.002			88	-94.7	478.7	13.814	0.003	1.343	0.005	1.520	0.062
15	97.1	130.4	14.040	0.006	0.466	0.007	0.060	0.023	89	-81.9	484.9	13.976	0.004	1.670	0.008	0.881	0.041
16	142.7	178.0	12.129	0.002	0.331	0.003	0.362	0.026	90	-43.2	486.5	13.470	0.003	1.801	0.004	2.123	0.065
17	117.1	118.1	12.787	0.002	0.567	0.003	0.212	0.009	91	250.4	515.3	13.680	0.003	1.714	0.006	2.059	0.157
18	163.0	99.1	13.175	0.002	0.577	0.003	0.051	0.008	92	328.5	465.1	13.665	0.002	0.633	0.004	0.266	0.016
19	144.4	-23.6	13.151	0.001	1.716	0.005	1.934	0.072	93	397.5	281.2	12.860	0.002	1.660	0.004	2.230	0.091
20	183.8	-74.7	13.127	0.002	0.661	0.004	0.154	0.011	94	436.7	181.5	12.917	0.002	0.477	0.003	0.028	0.008
21	190.3	-101.1	12.258	0.003	0.680	0.004	0.219	0.005	95	507.7	108.0	12.758	0.001	1.101	0.002	0.905	0.016
22	140.3	-71.3	12.691	0.002	1.068	0.004	1.007	0.014	96	553.7	-15.3	13.370	0.002	0.945	0.004	0.862	0.021
23	105.5	-81.6	12.352	0.002	0.363	0.003	0.080	0.004	97	548.3	-31.9	13.717	0.002	1.560	0.006	1.756	0.142
24	128.4	-140.8	11.282	0.003	1.548	0.004	1.948	0.012	98	505.0	-21.1	11.431	0.002	0.653	0.004	0.259	0.006
25	116.5	-183.2	12.948	0.002	0.603	0.004	0.091	0.008	99	348.8	-315.0	13.697	0.002	1.535	0.007	1.894	0.088
26	85.3	-170.2	13.932	0.002	0.646	0.004	0.071	0.015	105	-94.0	-478.3	13.523	0.002	1.314	0.004	1.305	0.021
27	58.5	-194.1	9.830	0.001	0.051	0.002	-0.452	0.005	107	-232.1	-498.0	11.536	0.002	0.228	0.003	0.086	0.002
28	24.4	-195.1	13.701	0.004	1.389	0.006	1.654	0.037	108	-344.5	-417.3	11.660	0.002	1.666	0.004	1.945	0.011
29	-115.5	-131.2	13.817	0.003	0.679	0.004	0.206	0.009	109	-376.5	-378.9	12.158	0.002	1.132	0.003	0.907	0.006
30	-141.6	-36.7	13.607	0.002	0.631	0.004	0.078	0.008	110	-446.9	-274.6	13.380	0.002	1.896	0.004	2.220	0.060
31	-157.5	-12.4	13.119	0.002	1.720	0.004	2.146	0.048	111	-510.2	-202.6	12.341	0.003	0.418	0.004	0.021	0.003
33	-179.8	45.4	9.893	0.001	0.037	0.003	-0.248	0.007	112	-445.5	-114.7	13.231	0.002	0.603	0.004	-0.024	0.005
34	-141.8	85.0	12.691	0.002	1.241	0.003	1.210	0.012	113	-454.6	-91.9	13.516	0.003	0.862	0.004	0.331	0.009
35	-150.3	105.5	13.528	0.003	0.581	0.004	0.044	0.008	201	-19.7	20.1	15.259	0.005	0.761	0.009	0.249	0.025
36	-76.0	138.5	13.059	0.003	0.574	0.004	0.097	0.005	202	-38.1	23.1	15.466	0.005	1.006	0.009	0.436	0.043
37	-121.8	146.9	11.768	0.002	0.323	0.002	0.138	0.002	203	-19.2	65.6	15.069	0.005	0.678	0.006	0.189	0.028
38	-102.1	169.3	11.774	0.003	0.317	0.003	0.126	0.003	204	59.4	-21.1	15.196	0.004	0.867	0.007	0.485	0.031
39	-48.0	276.0	12.735	0.003	1.222	0.004	1.280	0.014	205	83.2	-14.7	15.403	0.004	1.001	0.017		
40	-40.8	299.5	13.509	0.003	1.463	0.004	1.446	0.030	206	84.2	7.1	15.057	0.005	0.705	0.010	0.195	0.043
41	-44.3	337.5	11.255	0.003	0.179	0.004	0.032	0.002	207	78.3	38.6	14.597	0.002	1.186	0.005		
43	274.7	136.4	13.605	0.001	1.300	0.003	1.456	0.069	208	61.3	154.2	15.084	0.003	0.506	0.004	-0.076	0.044
44	278.3	53.3	13.186	0.002	1.486	0.003	1.553	0.060	209	43.7	83.0	14.740	0.004	0.805	0.006	0.283	0.056
45	244.4	-59.7	12.815	0.002	1.415	0.004	1.701	0.031	210	-14.0	96.3	15.393	0.006	1.239	0.009	1.295	0.125
46	232.1	-111.6	8.293	0.005	0.000	0.007	-0.410	0.006	211	-51.2	82.5	15.394	0.005	1.107	0.008	0.679	0.071
47	206.2	-180.1	11.455	0.002	0.193	0.003	0.050	0.003	212	-85.5	51.4	14.300	0.002	1.643	0.005	1.949	0.114
48	242.1	-218.6	13.743	0.002	1.560	0.006	1.986	0.106	213	-84.8	41.4	14.892	0.003	1.665	0.006		
49	53.1	-280.6	12.924	0.001	1.682	0.003	2.094	0.058	214	-109.2	3.2	14.461	0.003	1.242	0.006	1.450	0.098
50	-44.3	-317.8	13.291	0.003	1.374	0.004	1.626	0.026	215	-75.5	-69.1	14.248	0.003	0.619	0.005	0.089	0.011
51	-64.6	-290.0	10.484	0.002	1.754	0.003	2.174	0.006	216	-36.3	-76.5	15.469	0.007	1.540	0.014		
52	-212.9	-179.7	13.476	0.002	1.072	0.004	0.669	0.012	220	90.5	-95.9	14.489	0.005	0.727	0.009	0.408	0.030
53	-217.1	-75.1	13.875	0.003	1.361	0.005	1.499	0.034	221	96.4	-125.4	15.226	0.004	0.983	0.012	0.689	0.081
54	-249.8	97.7	13.191	0.003	0.557	0.004	0.088	0.006	222	134.0	-35.5	14.342	0.002	0.681	0.005	0.239	0.021
55	-181.5	138.4	9.248	0.003	0.029	0.004	-0.362	0.005	223	147.5	32.4	15.227	0.003	1.118	0.009		
56	-224.0	214.5	13.372	0.002	1.388	0.003	1.612	0.036	224	179.7	32.9	14.348	0.003	0.698	0.005	0.291	0.076
58	-22.3	444.2	11.684	0.004	0.990	0.004	0.648	0.004	225	138.2	75.6	14.820	0.003	1.148	0.007		
59	132.2	396.4	12.905	0.003	0.727	0.004	0.388	0.010	227	77.1	145.8	14.554	0.002	0.596	0.004	0.218	0.034
60	382.4	244.0	13.660	0.004	1.400	0.008	1.522	0.076	229	13.5	215.7	15.337	0.004	1.177	0.007		
61	291.0	186.6	13.978	0.002	1.067	0.004	0.636	0.043	230	-64.8	180.3	15.897	0.006	1.159	0.010	0.903	0.111
62	344.7	148.3	12.456	0.001	1.380	0.002	1.651	0.025	231	-111.4	152.2	14.664	0.004	1.479	0.007	1.857	0.069
63	402.7	171.0	13.822	0.002	1.059	0.004	0.684	0.030	232	-26.2	115.1	15.018	0.005	0.892	0.006	0.587	0.041
64	428.6	94.6	12.676	0.001													

Table 1. Photometric Data in NGC 6716 - Continue

ID	$\Delta\alpha(^{\prime\prime})$	$\Delta\delta(^{\prime\prime})$	V	ϵ_V	B-V	ϵ_{B-V}	U-B	ϵ_{U-B}	ID	$\Delta\alpha(^{\prime\prime})$	$\Delta\delta(^{\prime\prime})$	V	ϵ_V	B-V	ϵ_{B-V}	U-B	ϵ_{U-B}
246	209.2	224.4	14.709	0.004	0.577	0.006	0.109	0.035	326	-90.7	427.0	15.106	0.008	1.164	0.010	1.000	0.070
247	179.8	234.2	14.154	0.003	0.882	0.006	0.547	0.041	327	-118.3	411.0	15.205	0.004	0.661	0.006	0.241	0.029
249	138.0	225.3	15.618	0.007	1.287	0.028			328	-181.8	443.5	15.534	0.006	1.397	0.010	1.009	0.130
251	123.8	248.0	14.274	0.003	1.222	0.007	1.325	0.103	329	-204.5	323.8	14.624	0.003	0.822	0.005	0.354	0.020
252	49.0	267.6	15.032	0.003	1.226	0.005	0.660	0.131	330	-238.4	361.4	15.037	0.004	1.106	0.010	0.798	0.052
253	62.4	277.4	15.452	0.004	1.036	0.007	0.825	0.176	331	-246.6	342.1	15.137	0.007	1.253	0.014		
254	80.9	311.6	15.359	0.004	1.019	0.007			332	-300.1	292.2	15.276	0.007	0.734	0.009	0.188	0.030
255	98.3	325.9	14.266	0.004	0.765	0.006	0.255	0.030	333	-288.2	275.9	14.448	0.004	0.580	0.005	0.044	0.013
256	-13.2	243.9	15.347	0.004	0.770	0.006	0.289	0.034	336	-403.0	152.3	14.889	0.004	1.175	0.006	1.069	0.061
257	-43.6	263.7	15.181	0.007	1.208	0.010	0.908	0.069	337	-420.1	157.8	14.813	0.005	1.085	0.007	0.876	0.045
258	-24.4	279.0	14.218	0.003	1.382	0.005	1.582	0.060	339	-417.0	97.2	14.591	0.004	1.582	0.006		
259	-61.6	300.9	15.498	0.006	1.050	0.008	1.073	0.084	340	-414.0	40.0	15.109	0.003	1.163	0.006	0.620	0.065
260	-127.0	252.4	14.011	0.004	0.684	0.005	0.181	0.010	341	-388.7	21.2	13.988	0.004	1.400	0.006	1.485	0.043
261	-137.2	191.5	15.428	0.007	0.878	0.014	0.283	0.039	344	-369.0	-139.2	15.115	0.004	0.770	0.006	0.181	0.024
262	-180.6	192.3	14.876	0.006	1.083	0.008	0.932	0.049	345	-370.9	-194.8	14.906	0.004	0.771	0.006	0.296	0.021
263	-213.1	180.8	15.434	0.007	1.293	0.010	1.688	0.172	346	-355.0	-199.6	14.487	0.004	0.821	0.006	0.425	0.017
264	-267.3	177.9	15.259	0.007	1.223	0.010	1.162	0.084	347	-294.7	-291.9	15.143	0.005	0.696	0.008	0.116	0.022
265	-288.9	95.4	14.518	0.005	1.177	0.006	1.089	0.043	348	-281.1	-272.0	14.719	0.003	1.113	0.007	0.735	0.032
266	-268.0	100.2	15.342	0.005	1.183	0.008	1.017	0.083	349	-249.8	-257.1	13.778	0.003	0.494	0.004	0.427	0.010
267	-273.7	92.0	15.300	0.005	1.294	0.008	1.903	0.175	350	-274.5	-286.2	14.441	0.003	1.260	0.006	1.300	0.043
268	-324.9	60.4	14.870	0.003	1.014	0.005	0.497	0.036	352	-242.3	-284.7	15.641	0.006	1.043	0.011	0.483	0.059
269	-263.4	48.5	14.838	0.003	1.254	0.005	1.567	0.101	353	-176.4	-330.3	14.053	0.004	1.600	0.006	1.840	0.064
270	-251.4	28.1	14.126	0.002	0.563	0.003	0.234	0.017	354	-138.9	-337.6	15.176	0.004	1.098	0.008	0.721	0.048
271	-268.6	11.5	14.968	0.004	1.112	0.007			355	-47.0	-434.7	14.778	0.004	0.582	0.006	0.055	0.015
272	-268.9	-13.3	14.969	0.004	1.789	0.010			356	-21.3	-438.1	14.782	0.004	1.159	0.007	1.312	0.056
273	-285.7	-21.5	15.176	0.004	0.889	0.008	0.506	0.036	357	-6.7	-424.1	14.645	0.004	1.119	0.006	1.013	0.038
274	-241.4	-175.2	14.372	0.003	0.777	0.006	0.346	0.015	358	-7.8	-400.9	15.326	0.004	1.330	0.009	1.332	0.119
275	-227.9	-220.2	14.630	0.004	1.279	0.007	1.147	0.049	359	-43.7	-358.9	14.097	0.003	1.177	0.005	0.901	0.021
276	-160.2	-221.2	15.489	0.006	1.484	0.011	1.475	0.162	360	13.5	-370.8	14.421	0.004	0.671	0.006	0.143	0.015
277	-147.6	-250.1	15.191	0.009	0.991	0.013	0.599	0.034	361	26.2	-378.8	14.463	0.003	1.149	0.006	1.163	0.038
279	-89.2	-220.2	15.203	0.004	1.517	0.009	1.594	0.132	362	62.4	-368.6	14.606	0.003	0.713	0.007	0.144	0.035
281	-125.5	-287.9	14.892	0.004	0.889	0.007	0.293	0.025	363	112.0	-380.3	14.024	0.004	0.746	0.009	0.223	0.021
282	-86.0	-298.0	14.266	0.003	0.767	0.005	0.184	0.012	365	179.2	-387.5	15.767	0.009	1.094	0.025		
283	11.4	-334.7	15.313	0.005	1.351	0.010			366	207.5	-393.5	14.116	0.003	0.587	0.006	0.104	0.025
284	53.2	-322.4	14.181	0.002	0.714	0.004	0.099	0.019	368	265.0	-357.1	14.218	0.003	0.786	0.006	0.404	0.026
286	26.4	-279.8	14.490	0.003	0.746	0.005	0.318	0.017	370	330.6	-387.8	14.309	0.003	0.685	0.006	0.159	0.021
287	95.9	-230.1	14.404	0.003	1.312	0.009	1.408	0.098	372	382.1	-377.4	13.999	0.002	1.692	0.007	1.983	0.159
288	113.7	-231.7	15.058	0.004	1.065	0.012	0.725	0.079	373	399.4	-323.9	14.030	0.002	0.665	0.004	0.091	0.015
289	209.6	-224.9	15.201	0.004	0.840	0.011	0.296	0.054	374	420.4	-321.8	14.987	0.004	1.611	0.015	2.016	0.336
291	251.2	-252.8	13.829	0.002	0.915	0.005	0.622	0.037	375	407.1	-305.0	14.847	0.003	1.292	0.010	1.320	0.128
292	280.4	-232.4	15.189	0.004	0.768	0.010	0.283	0.051	376	507.4	-267.7	14.462	0.002	1.111	0.007	0.831	0.079
293	330.4	-306.0	14.798	0.003	0.769	0.008	0.279	0.038	377	411.0	-249.7	14.298	0.002	1.027	0.006	0.705	0.037
294	344.1	-232.9	13.999	0.002	0.626	0.004	0.161	0.016	378	421.9	-240.2	15.051	0.004	1.237	0.012	0.974	0.107
295	361.6	-239.1	15.103	0.004	0.797	0.010	0.581	0.062	379	461.6	-235.7	14.477	0.002	1.492	0.009	2.038	0.204
296	375.7	-240.0	14.457	0.003	1.384	0.011			380	428.3	-185.6	14.812	0.003	1.290	0.010	1.547	0.369
297	398.0	-202.2	15.124	0.004	0.972	0.012	0.486	0.065	381	548.6	-151.0	14.812	0.003	0.930	0.009	0.335	0.044
298	345.8	-163.8	15.284	0.004	1.426	0.016			383	438.2	-124.9	14.224	0.003	0.876	0.008	0.455	0.032
299	345.3	-132.7	15.065	0.004	0.646	0.009	0.015	0.035	384	499.7	-107.6	14.967	0.003	1.624	0.015		
300	329.3	-125.4	14.647	0.003	1.125	0.009	1.018	0.093	385	535.7	-98.9	14.897	0.004	0.669	0.008	0.167	0.040
301	330.8	-119.4	15.041	0.006	1.363	0.015			386	504.1	-85.9	14.676	0.003	1.648	0.012		
302	410.9	-104.5	15.144	0.003	0.856	0.010	0.340	0.054	387	495.2	-88.2	14.705	0.003	1.175	0.009	0.677	0.066
303	416.9	-94.3	14.894	0.004	1.230	0.012			388	500.4	-72.5	14.157	0.003	1.332	0.007	1.869	0.214
307	427.8	62.3	14.976	0.003	0.763	0.006	0.406	0.056	389	469.0	-63.7	15.014	0.005	0.864	0.011	0.362	0.069
308	395.6	123.3	14.169	0.002	1.193	0.005	1.208	0.061	390	564.3	-13.2	14.656	0.003	0.672	0.007	0.153	0.030
309	430.9	117.0	14.522	0.002	0.746	0.005	0.350	0.030	391	531.4	87.1	13.948	0.001	1.380	0.005	1.439	0.076
310	341.8	120.7	15.000	0.002	1.026	0.007	0.796	0.084	392	461.1	104.3	15.797	0.008	1.168	0.023		
311	384.8	140.1	15.344	0.003	0.745	0.008	0.184	0.058	393	527.6	136.3	14.717	0.002	0.778	0.005	0.318	0.039
312	311.7	193.8	14.816	0.002	0.552	0.006			394	517.3	152.0	14.954	0.003	1.151	0.009	0.719	0.083
313	279.3	248.9	15.307	0.005	0.652	0.010	0.158	0.064	395	484.8	154.0	14.532	0.002	0.970	0.005	0.882	0.174
314	319.2	272.4	14.856	0.003	1.505	0.010			396	525.8	202.3</						

Table 1. Photometric Data in NGC 6716 - Continue

ID	$\Delta\alpha''$	$\Delta\delta''$	V	ϵ_V	B-V	ϵ_{B-V}	U-B	ϵ_{U-B}	ID	$\Delta\alpha''$	$\Delta\delta''$	V	ϵ_V	B-V	ϵ_{B-V}	U-B	ϵ_{U-B}
407	275.0	442.5	14.695	0.003	1.736	0.011	1.241	0.191	1306	-231.4	-432.6	15.832	0.014	1.192	0.022	0.729	0.099
409	248.0	471.7	14.684	0.003	1.177	0.009	0.886	0.103	1309	-417.7	-432.4	11.817	0.002	0.605	0.004	0.127	0.004
410	245.9	505.1	15.471	0.007	1.497	0.020			1332	-1.9	-425.0	15.515	0.006	0.967	0.010	0.667	0.057
411	165.2	507.7	14.770	0.004	1.270	0.009	1.119	0.166	1340	-494.4	-423.1	15.489	0.007	1.450	0.013	0.766	0.136
412	87.6	511.4	14.920	0.004	1.052	0.011			1342	594.4	-422.9	14.346	0.006	0.650	0.009	-0.036	0.025
414	65.1	494.7	15.178	0.004	0.710	0.006	0.061	0.056	1349	-107.8	-420.8	15.884	0.007	1.080	0.012	1.556	0.138
415	38.3	477.7	15.178	0.004	0.801	0.006	0.487	0.083	1350	-265.7	-420.5	15.224	0.005	1.407	0.009		
416	61.2	553.3	15.299	0.004	1.076	0.007	0.320	0.169	1353	544.6	-420.2	14.824	0.005	1.094	0.012	0.965	0.246
417	62.1	560.8	15.084	0.005	1.138	0.007	0.905	0.155	1356	-196.6	-419.4	12.622	0.002	0.499	0.003	0.044	0.004
419	9.8	574.9	15.390	0.005	1.539	0.009			1366	417.0	-417.1	15.365	0.004	1.199	0.015	1.445	0.216
420	-27.9	536.8	14.105	0.003	1.380	0.005	1.332	0.046	1370	-217.3	-416.6	15.417	0.005	1.126	0.009		
421	-49.4	564.5	15.259	0.005	1.146	0.008	0.769	0.069	1371	92.7	-416.6	15.823	0.007	0.768	0.017	-0.162	0.082
422	-109.8	544.9	14.417	0.003	0.718	0.004	0.078	0.015	1378	229.3	-414.6	15.869	0.008	1.044	0.020	0.406	0.152
423	-118.6	519.9	14.402	0.003	1.640	0.006	2.101	0.135	1389	-7.6	-411.8	15.879	0.015	0.800	0.022	0.139	0.048
424	-209.9	493.4	15.198	0.008	1.412	0.018	1.382	0.115	1396	633.5	-410.6	15.731	0.007	0.703	0.017	0.328	0.145
425	-206.1	503.8	13.924	0.003	0.582	0.004	1.707	0.466	1416	527.4	-406.9	15.923	0.009	0.975	0.022		
426	-213.7	533.0	14.512	0.005	1.010	0.006	0.848	0.031	1419	584.4	-406.7	15.843	0.006	1.087	0.022		
427	-275.9	400.2	14.694	0.004	1.290	0.006	1.199	0.060	1421	6.7	-406.1	15.634	0.006	0.950	0.010	0.359	0.052
428	-265.5	385.0	15.155	0.009	1.088	0.011	0.791	0.049	1428	309.4	-404.9	15.434	0.005	0.765	0.012	0.341	0.076
430	-361.6	382.3	15.100	0.004	0.798	0.006	0.361	0.030	1429	515.7	-404.7	15.667	0.006	1.041	0.018	1.037	0.187
432	-333.3	346.7	14.581	0.004	1.357	0.006	1.349	0.103	1444	221.2	-402.3	15.619	0.005	1.136	0.017	0.576	0.140
433	-341.4	329.0	14.417	0.003	1.307	0.007	1.283	0.047	1459	447.8	-400.0	14.443	0.003	1.056	0.009	1.298	0.085
435	-459.6	300.8	15.004	0.004	0.888	0.006	0.448	0.031	1461	-441.3	-399.7	15.350	0.005	0.890	0.009	0.297	0.035
436	-428.4	286.7	15.108	0.005	0.929	0.006	0.179	0.027	1469	151.6	-398.9	15.454	0.007	0.656	0.014	0.094	0.061
439	-453.6	198.1	14.806	0.005	0.754	0.006	0.316	0.025	1476	229.7	-398.1	14.940	0.003	1.028	0.010	0.722	0.077
440	-456.7	190.9	15.423	0.009	0.902	0.020			1496	194.7	-395.2	15.489	0.005	1.205	0.018	0.940	0.186
443	-461.7	136.5	14.969	0.004	1.341	0.006	1.104	0.072	1497	-136.8	-395.0	15.724	0.005	1.184	0.010	0.687	0.066
444	-486.5	24.3	14.885	0.006	0.842	0.008	0.196	0.023	1499	-148.6	-394.7	15.955	0.007	1.103	0.013	0.929	0.094
445	-537.8	-10.8	15.594	0.010	1.320	0.016			1507	433.1	-392.6	15.343	0.005	1.095	0.015	0.859	0.121
446	-477.9	-51.8	14.992	0.004	1.620	0.008	1.556	0.115	1515	-170.4	-390.9	15.758	0.011	0.838	0.016	0.245	0.044
447	-534.3	-90.4	14.773	0.006	0.766	0.017	0.301	0.028	1518	-424.5	-390.3	15.288	0.004	1.411	0.009		
448	-473.4	-69.5	15.447	0.007	1.336	0.012			1526	-261.9	-389.0	15.922	0.006	1.260	0.013		
449	-515.1	-173.3	15.011	0.004	1.110	0.007	0.761	0.045	1545	198.1	-385.8	15.552	0.005	0.906	0.014	1.254	0.180
451	-451.3	-234.5	15.267	0.011	0.813	0.014	0.184	0.029	1547	177.0	-385.5	15.772	0.007	0.602	0.017	0.367	0.320
452	-441.4	-247.8	14.838	0.006	0.995	0.009	0.501	0.029	1549	631.6	-385.4	15.301	0.006	0.645	0.013	0.008	0.049
453	-449.1	-324.2	14.495	0.004	0.829	0.006	0.225	0.016	1551	118.1	-385.3	15.241	0.005	1.120	0.014		
454	-398.5	-388.7	15.191	0.005	1.467	0.009	1.372	0.108	1576	-434.8	-380.1	15.531	0.006	1.467	0.012		
456	-331.2	-337.5	14.464	0.005	1.172	0.008	1.081	0.040	1606	-230.4	-375.3	15.390	0.004	0.697	0.007	0.059	0.025
457	-315.7	-388.5	14.653	0.004	1.405	0.007	1.435	0.074	1623	266.1	-372.4	15.088	0.004	0.850	0.010	0.476	0.055
458	-322.2	-418.4	14.964	0.005	0.888	0.007	0.380	0.025	1630	492.7	-370.5	15.242	0.006	0.799	0.011	0.286	0.085
459	-284.7	-486.7	14.747	0.005	1.263	0.008	1.067	0.046	1632	-190.5	-370.3	15.788	0.006	0.861	0.010	0.432	0.052
460	-266.5	-485.7	13.990	0.003	1.271	0.008	1.224	0.031	1652	497.0	-366.7	12.773	0.003	1.021	0.004	0.700	0.015
461	-99.3	-513.5	14.856	0.004	1.222	0.007	1.011	0.048	1670	594.4	-362.5	15.912	0.007	1.184	0.024		
463	-54.7	-513.5	15.142	0.005	1.503	0.010	1.677	0.217	1681	583.4	-360.7	15.185	0.004	0.708	0.010	0.026	0.045
464	-48.3	-482.7	15.022	0.008	0.812	0.012	0.275	0.026	1684	148.1	-359.8	15.316	0.004	0.755	0.011	0.261	0.063
465	-25.5	-474.7	14.959	0.005	1.249	0.009	1.044	0.059	1685	190.8	-359.1	15.661	0.006	0.873	0.015	0.416	0.098
1004	-284.6	-553.1	14.441	0.004	1.818	0.007	2.002	0.147	1702	-153.2	-356.6	15.821	0.006	0.653	0.010	0.003	0.032
1020	-417.7	-543.0	14.656	0.005	1.411	0.009			1711	554.1	-355.2	15.223	0.004	1.140	0.013	1.069	0.137
1031	-236.9	-539.2	13.476	0.003	0.816	0.004	0.390	0.010	1723	-491.2	-352.8	14.675	0.004	1.144	0.006	0.875	0.037
1032	-479.3	-539.2	15.606	0.007	0.724	0.011	0.094	0.044	1726	-425.9	-352.2	15.732	0.006	1.211	0.011	0.923	0.102
1042	-220.4	-536.1	15.513	0.007	1.048	0.015	0.769	0.074	1727	394.4	-351.8	15.510	0.004	0.834	0.014	0.566	0.087
1043	-242.3	-536.0	15.453	0.005	0.914	0.009	0.482	0.048	1739	-311.0	-351.1	15.651	0.005	1.033	0.009	0.815	0.075
1065	-414.6	-528.2	14.889	0.004	1.169	0.007	0.938	0.062	1743	161.3	-350.0	14.884	0.004	1.282	0.013	1.278	0.138
1069	-212.4	-526.6	15.526	0.006	1.005	0.010	0.829	0.065	1748	190.7	-349.1	15.795	0.006	0.760	0.016	0.433	0.105
1070	-89.2	-526.5	15.617	0.006	0.896	0.010	0.429	0.054	1751	-16.9	-348.3	15.645	0.008	0.392	0.010	0.103	0.024
1115	-339.7	-501.9	15.556	0.005	1.082	0.009	0.699	0.068	1754	122.6	-347.9	15.768	0.006	0.907	0.018		
1117	-160.1	-501.2	15.386	0.006	0.880	0.009			1775	516.0	-342.6	14.247	0.003	1.269	0.008	1.202	0.072
1127	52.7	-498.5	15.934	0.008	1.131	0.015	0.598	0.098	1781	649.9	-341.5	15.266	0.006	0.637	0.012		
1154	-306.4	-488.5	15.930	0.008	0.854	0.012	0.310	0.058	1788	-494.4	-340.1	15.805	0.008	0.807	0.011	0.268	0.052
1164	41.6	-486.1	15.747	0.006	1.090	0.012	0.687	0.093	1836	-92.4							

Table 1. Photometric Data in NGC 6716 - Continue

ID	$\Delta\alpha(^{\prime\prime})$	$\Delta\delta(^{\prime\prime})$	V	ϵ_V	B-V	ϵ_{B-V}	U-B	ϵ_{U-B}	ID	$\Delta\alpha(^{\prime\prime})$	$\Delta\delta(^{\prime\prime})$	V	ϵ_V	B-V	ϵ_{B-V}	U-B	ϵ_{U-B}
1950	521.9	-312.4	14.585	0.003	1.346	0.010	1.780	0.159	3262	-240.0	-72.5	15.994	0.006	1.331	0.013		
1964	-379.5	-310.3	15.995	0.006	0.905	0.010			3273	504.9	-71.0	15.823	0.007	0.967	0.019	0.041	0.085
1996	-542.6	-304.5	15.301	0.005	0.823	0.008	0.247	0.034	3282	24.8	-69.1	14.883	0.004	1.005	0.007	0.611	0.030
2021	163.0	-300.6	15.906	0.006	1.126	0.023			3299	156.2	-65.4	15.428	0.005	0.901	0.013	0.783	0.099
2029	121.2	-299.4	15.431	0.006	1.064	0.016			3320	23.1	-62.0	14.475	0.003	1.450	0.007		
2046	-370.0	-297.1	15.424	0.005	1.202	0.009	1.374	0.100	3321	620.6	-62.0	12.593	0.002	0.402	0.004	0.064	0.006
2049	414.5	-297.0	15.504	0.006	1.153	0.018	0.927	0.147	3348	210.9	-56.0	15.783	0.007	1.314	0.024	0.585	0.195
2056	-255.4	-295.5	15.327	0.005	0.832	0.008	0.233	0.030	3363	-529.2	-53.2	15.538	0.006	1.354	0.011	1.277	0.128
2085	-142.3	-290.8	15.178	0.007	0.928	0.010	0.663	0.059	3371	-318.9	-51.8	15.932	0.006	0.835	0.011	0.263	0.045
2117	200.2	-284.5	15.156	0.004	1.129	0.013	1.189	0.145	3385	163.0	-48.9	15.944	0.006	0.901	0.019	0.516	0.126
2228	219.0	-265.0	14.657	0.004	1.273	0.011	1.126	0.100	3386	-199.0	-48.8	15.694	0.006	0.682	0.009	0.061	0.035
2250	-404.4	-260.3	15.345	0.006	0.763	0.008	0.259	0.029	3387	-210.5	-48.8	15.881	0.006	1.154	0.012		
2274	-230.6	-257.1	15.968	0.006	1.011	0.012			3439	-536.0	-39.1	15.068	0.007	1.154	0.010	0.391	0.041
2291	-288.7	-254.7	15.767	0.006	0.707	0.009	0.108	0.034	3454	596.4	-37.1	15.463	0.004	1.205	0.016		
2313	385.0	-250.5	15.949	0.008	0.799	0.018	0.173	0.095	3461	-195.6	-35.7	15.721	0.006	1.374	0.013		
2340	206.8	-245.7	15.921	0.006	1.228	0.024			3466	550.6	-35.4	15.351	0.004	1.316	0.017	1.900	0.369
2382	263.2	-239.4	15.577	0.007	0.751	0.014	0.255	0.068	3481	-346.9	-32.2	15.493	0.006	1.247	0.011		
2394	144.8	-238.3	15.507	0.005	0.747	0.013	0.378	0.073	3498	168.0	-28.8	15.117	0.003	0.785	0.010	0.161	0.053
2401	-169.7	-236.6	15.978	0.006	0.824	0.011			3522	502.1	-25.2	14.747	0.011	1.259	0.024	0.182	0.112
2413	-471.2	-234.4	15.866	0.016	0.982	0.025	0.218	0.056	3525	279.8	-25.0	15.772	0.006	1.129	0.021		
2416	568.4	-234.2	15.938	0.007	0.582	0.016	-0.301	0.059	3527	121.0	-24.6	15.991	0.009	1.141	0.026	0.524	0.175
2436	-337.8	-231.1	15.609	0.006	1.600	0.017			3543	106.0	-22.4	15.749	0.006	0.769	0.015	0.183	0.071
2460	-292.5	-227.5	15.751	0.007	1.465	0.014	1.002	0.120	3549	-341.1	-21.0	14.495	0.003	1.290	0.006	1.133	0.043
2468	-406.3	-226.1	15.423	0.005	0.868	0.008	0.425	0.039	3554	378.8	-19.4	15.636	0.006	0.805	0.015	0.311	0.084
2486	135.8	-222.6	15.736	0.005	0.874	0.016	0.614	0.117	3557	138.3	-19.0	15.810	0.005	0.766	0.013	0.087	0.088
2488	-401.7	-222.1	15.458	0.005	1.174	0.009	1.129	0.086	3558	652.4	-18.9	15.070	0.003	1.301	0.012		
2495	288.4	-220.4	15.625	0.006	0.669	0.015	0.114	0.066	3596	585.9	-11.5	15.449	0.006	0.846	0.014	0.531	0.090
2536	226.4	-214.9	15.645	0.006	0.153	0.011	-0.347	0.029	3615	496.1	-8.5	15.902	0.007	0.993	0.020	0.505	0.123
2545	562.0	-213.2	15.424	0.004	1.282	0.017			3620	-40.0	-7.3	15.872	0.008	0.930	0.013	0.431	0.063
2546	513.0	-213.2	15.770	0.005	1.357	0.023			3627	79.3	-6.5	15.958	0.006	0.771	0.017	0.132	0.094
2614	607.5	-201.1	9.828	0.005	-0.027	0.007	-0.453	0.006	3628	130.5	-6.4	15.382	0.004	0.908	0.013	0.442	0.074
2622	-436.4	-199.5	15.516	0.007	0.911	0.011	0.469	0.043	3629	579.6	-6.2	14.970	0.004	0.758	0.010	0.257	0.045
2625	-422.3	-199.2	15.294	0.004	1.049	0.008	0.275	0.036	3642	118.7	-4.6	15.992	0.007	1.011	0.023	0.710	0.179
2643	624.6	-195.4	15.484	0.005	0.595	0.012	-0.046	0.098	3646	-493.6	-3.7	15.845	0.009	1.220	0.014		
2664	98.8	-192.7	15.509	0.005	1.357	0.019			3648	-218.6	-3.3	15.547	0.006	0.695	0.009	0.182	0.034
2667	-196.8	-191.6	15.298	0.005	0.849	0.008	0.425	0.033	3652	570.7	-2.7	14.995	0.003	1.434	0.013	1.242	0.192
2693	89.8	-185.4	15.959	0.006	1.098	0.021	0.679	0.179	3653	414.7	-2.7	15.801	0.006	0.743	0.016	0.288	0.085
2697	66.8	-185.1	15.561	0.013	0.618	0.019			3662	218.4	-1.0	15.975	0.007	1.169	0.022	0.823	0.231
2715	-389.6	-181.7	15.916	0.010	1.379	0.015	1.580	0.236	3665	-493.8	-0.2	15.483	0.010	1.030	0.013	-0.002	0.041
2717	155.7	-181.6	15.480	0.007	0.908	0.016	0.334	0.075	3688	468.7	2.9	15.324	0.005	0.810	0.013	0.484	0.104
2766	36.9	-173.7	15.984	0.006	1.012	0.012	1.007	0.125	3689	126.0	3.0	15.729	0.006	1.041	0.017	0.949	0.185
2767	296.2	-173.4	15.889	0.006	1.192	0.021			3713	343.9	7.9	15.689	0.016	1.224	0.064	-0.024	0.111
2786	286.9	-170.2	15.642	0.005	0.833	0.014	0.269	0.078	3716	580.5	8.3	15.475	0.004	1.007	0.016	0.556	0.110
2792	-480.0	-168.0	15.814	0.009	1.386	0.016	1.073	0.144	3729	157.7	9.7	15.596	0.006	0.802	0.015	0.174	0.073
2804	-462.1	-164.6	15.541	0.005	0.680	0.008	-0.036	0.029	3739	312.5	11.5	15.774	0.005	1.140	0.018		
2823	456.3	-161.5	15.690	0.005	1.136	0.018	0.973	0.203	3771	-212.3	16.0	15.894	0.006	1.257	0.012		
2860	75.9	-153.6	15.865	0.005	1.128	0.021	0.641	0.167	3788	-248.4	19.4	15.828	0.006	0.884	0.010		
2882	54.0	-149.7	15.857	0.006	0.872	0.010	0.823	0.168	3793	-188.3	20.7	11.150	0.002	0.215	0.005	-0.074	0.006
2963	-464.7	-134.2	15.631	0.005	1.196	0.010			3799	632.6	21.6	14.838	0.003	1.339	0.011	1.366	0.141
3005	619.2	-126.4	13.649	0.002	1.147	0.006	1.271	0.044	3801	-508.1	21.9	15.808	0.009	0.645	0.012	-0.206	0.033
3016	279.2	-123.9	15.665	0.005	1.325	0.020	1.394	0.287	3804	-462.0	22.4	15.032	0.005	1.377	0.009	1.200	0.082
3018	419.6	-123.6	14.226	0.002	1.382	0.011	1.576	0.091	3817	479.4	23.8	15.763	0.008	0.794	0.017	0.452	0.092
3033	626.8	-120.6	14.848	0.004	1.315	0.011			3820	-277.1	24.3	15.757	0.011	0.862	0.015	0.291	0.049
3048	443.4	-117.8	13.190	0.008	0.549	0.009	0.059	0.009	3838	-345.9	27.6	15.661	0.006	1.169	0.011	1.151	0.111
3067	318.0	-113.8	15.800	0.007	0.710	0.016	0.294	0.078	3839	198.7	27.7	15.758	0.004	0.751	0.010		
3069	631.6	-113.7	15.578	0.005	1.231	0.019			3858	-73.8	30.3	15.859	0.005	1.021	0.008	0.675	0.106
3080	-496.3	-111.3	15.698	0.006	0.809	0.009	0.194	0.042	3866	473.5	31.9	15.878	0.004	1.173	0.015		
3091	309.3	-108.5	15.917	0.011	0.884	0.023	0.105	0.085	3875	630.1	33.6	15.653	0.007	0.842	0.017	0.462	0.091
3094	461.6	-108.2	15.606	0.007	1.293	0.021			3901	387.8	35.8	15.636	0.004	0.948	0.012		
3116	216.5	-105.0	14.664	0.004	1.400	0.013			3911	-310.3	37.2	15.610	0.004	0.758	0.006	0.156	0.047
3135	-162.1	-101.3	15.925														

Table 1. Photometric Data in NGC 6716 - Continue

ID	$\Delta\alpha''$	$\Delta\delta''$	V	ϵ_V	B-V	ϵ_{B-V}	U-B	ϵ_{U-B}	ID	$\Delta\alpha''$	$\Delta\delta''$	V	ϵ_V	B-V	ϵ_{B-V}	U-B	ϵ_{U-B}
4185	-110.4	70.3	15.952	0.008	1.468	0.014			5461	455.4	247.1	15.836	0.005	1.054	0.018	0.643	0.240
4205	61.4	73.1	15.675	0.007	0.799	0.012			5506	247.2	253.1	15.554	0.005	0.934	0.014	0.275	0.115
4225	62.8	75.9	14.984	0.005	0.671	0.008	-0.045	0.209	5510	-109.1	253.5	15.717	0.007	0.803	0.011	0.468	0.054
4237	130.4	77.9	15.895	0.005	1.075	0.014			5550	603.7	258.8	15.022	0.004	1.194	0.011	1.504	0.261
4251	-7.3	79.8	15.944	0.006	1.189	0.014			5581	585.3	262.6	14.244	0.003	0.963	0.006	0.776	0.057
4278	184.1	82.9	15.844	0.005	0.732	0.012	0.291	0.153	5606	314.7	265.0	15.720	0.006	0.840	0.014	0.561	0.150
4304	-247.9	85.8	15.806	0.011	0.849	0.015	0.736	0.098	5614	484.6	266.5	15.722	0.005	0.727	0.014	0.151	0.101
4357	-195.3	90.8	15.807	0.007	0.914	0.010	0.403	0.067	5626	-217.2	268.8	13.744	0.003	1.893	0.006	0.307	0.025
4369	631.1	92.3	15.387	0.005	0.845	0.014	0.493	0.128	5651	217.8	272.9	15.537	0.005	1.240	0.017	1.126	0.294
4371	625.9	92.5	15.789	0.006	0.682	0.016	0.256	0.124	5664	229.3	275.3	15.999	0.008	1.029	0.022	0.669	0.266
4376	-82.0	93.5	15.989	0.006	0.907	0.009	0.696	0.095	5709	-392.9	282.3	15.989	0.008	1.070	0.013	0.774	0.106
4392	-107.0	95.7	15.771	0.006	1.183	0.009	1.167	0.138	5731	117.8	285.2	15.609	0.006	0.753	0.013	0.040	0.080
4419	429.7	99.2	15.909	0.010	1.130	0.027			5788	514.8	294.5	15.154	0.004	0.772	0.009	0.080	0.057
4444	628.5	102.1	15.176	0.004	1.394	0.015			5791	49.7	294.8	15.930	0.005	0.798	0.008	0.203	0.142
4474	-152.4	106.5	15.912	0.019	0.722	0.034			5799	209.2	295.7	15.621	0.006	0.890	0.013	0.753	0.175
4488	617.2	109.0	14.407	0.004	1.238	0.009	1.342	0.083	5839	32.0	298.9	15.833	0.006	0.698	0.011		
4522	-333.6	115.0	15.854	0.006	1.160	0.010			5870	559.8	302.7	14.167	0.003	1.279	0.007	1.154	0.090
4542	132.8	117.2	15.809	0.005	1.116	0.014			5892	236.0	305.7	15.669	0.005	1.235	0.016		
4582	565.5	124.3	15.528	0.004	1.159	0.011			5931	340.3	310.8	15.931	0.006	1.179	0.030		
4597	-220.1	126.7	14.550	0.005	1.141	0.006	1.227	0.049	5969	583.3	315.2	15.143	0.004	0.832	0.009	0.381	0.087
4611	140.0	128.9	15.569	0.004	1.634	0.016			5977	385.8	315.9	15.574	0.005	1.143	0.015	0.831	0.213
4622	177.9	131.5	15.431	0.005	0.926	0.011	0.406	0.143	5982	572.6	316.8	15.479	0.004	0.758	0.011	0.420	0.112
4656	100.0	135.9	15.302	0.007	0.898	0.012	0.497	0.155	5989	439.8	317.9	15.346	0.007	0.781	0.013	0.531	0.099
4664	390.9	136.9	15.502	0.003	0.987	0.010	0.227	0.082	6013	-403.4	321.0	15.774	0.006	1.141	0.010	0.449	0.199
4673	180.5	138.2	15.437	0.004	1.107	0.011			6031	465.7	323.2	15.608	0.005	1.188	0.016	0.824	0.288
4688	-68.3	139.8	15.046	0.006	1.124	0.008	0.739	0.055	6036	137.0	323.4	14.929	0.004	1.410	0.012		
4694	-418.5	141.1	15.527	0.009	0.838	0.011	0.327	0.046	6097	474.7	331.5	14.981	0.004	0.817	0.008	0.299	0.058
4703	456.6	142.7	15.888	0.004	0.797	0.012	0.365	0.109	6111	610.1	333.5	14.920	0.004	0.934	0.008	0.734	0.097
4745	-151.4	148.4	15.743	0.007	0.739	0.009	0.305	0.042	6161	565.0	340.9	14.810	0.003	1.347	0.010	1.511	0.230
4755	593.7	149.9	15.602	0.004	0.867	0.010			6169	593.3	341.5	15.344	0.005	1.597	0.026		
4765	319.9	151.2	15.983	0.004	0.673	0.011	0.046	0.091	6196	520.5	345.7	15.804	0.006	0.934	0.016		
4779	451.8	153.2	15.937	0.005	0.851	0.013	0.568	0.155	6204	-316.1	346.9	15.524	0.006	1.095	0.008	0.957	0.085
4787	-395.6	154.0	15.697	0.006	0.866	0.008	0.608	0.068	6221	245.7	348.7	15.980	0.006	1.216	0.024		
4794	640.0	154.7	15.911	0.006	1.359	0.029			6230	509.3	350.1	13.451	0.002	0.584	0.004	0.176	0.028
4796	204.8	154.8	15.866	0.004	0.871	0.012	0.195	0.139	6238	-383.1	351.2	15.831	0.006	1.195	0.007	0.047	0.026
4814	157.5	158.2	14.600	0.002	0.595	0.005	0.171	0.039	6263	-18.0	353.9	15.610	0.009	1.253	0.014	1.116	0.137
4818	487.9	158.5	15.520	0.004	0.699	0.009	0.092	0.084	6264	-433.3	353.9	15.329	0.005	1.412	0.009	1.915	0.202
4825	150.5	159.1	14.578	0.002	0.660	0.005	0.152	0.035	6284	384.8	357.0	15.554	0.005	1.297	0.018		
4843	82.3	162.5	15.780	0.004	0.854	0.008			6332	-219.5	363.6	15.930	0.007	1.223	0.011		
4856	-21.7	164.9	15.912	0.008	0.988	0.011	0.791	0.097	6349	-283.4	366.7	15.106	0.007	1.428	0.010	1.476	0.109
4883	-313.9	167.3	15.919	0.006	0.961	0.010	0.431	0.075	6354	-296.1	367.3	15.400	0.006	1.191	0.008	1.279	0.108
4892	418.6	168.2	15.657	0.004	1.450	0.015			6365	169.6	368.9	15.591	0.010	0.637	0.015	0.117	0.075
4899	-54.8	169.1	15.529	0.007	0.953	0.011	0.629	0.065	6383	373.7	371.3	15.561	0.005	0.958	0.012		
4909	447.1	170.6	15.550	0.003	1.414	0.014			6389	203.0	372.4	15.557	0.005	1.124	0.014	0.729	0.172
4946	274.1	174.6	14.110	0.002	0.667	0.004	0.166	0.049	6395	466.7	373.0	15.474	0.005	1.018	0.015	0.226	0.111
4948	210.8	174.7	15.549	0.004	1.309	0.013			6429	575.4	377.8	15.265	0.005	0.937	0.011		
4956	559.3	175.6	15.554	0.004	1.116	0.012			6470	-179.0	382.0	15.429	0.007	1.514	0.012		
4967	270.1	176.7	15.424	0.004	1.021	0.010	0.582	0.163	6471	468.5	382.5	15.892	0.009	1.410	0.025		
5069	-282.0	191.5	14.879	0.004	0.767	0.007	0.012	0.022	6483	-470.4	383.8	15.114	0.004	1.565	0.007		
5071	-454.9	191.7	15.831	0.011	0.637	0.014	-0.621	0.028	6523	154.1	389.9	15.226	0.004	0.275	0.007	0.104	0.038
5075	170.5	191.9	15.863	0.004	0.781	0.011	0.027	0.110	6529	-387.5	390.2	15.470	0.005	1.115	0.009	0.881	0.079
5079	-284.5	192.3	15.662	0.008	1.081	0.016			6533	-408.4	390.6	15.288	0.013	0.957	0.016	0.598	0.053
5080	-423.2	192.4	15.515	0.005	0.704	0.007	0.118	0.036	6537	217.1	391.3	15.859	0.006	1.453	0.023		
5086	558.2	193.5	14.668	0.002	0.804	0.007			6538	-139.0	391.3	15.911	0.007	1.406	0.013		
5091	41.7	194.2	15.890	0.009	1.071	0.015			6575	-179.8	395.3	15.892	0.007	1.623	0.013		
5124	203.9	199.1	15.224	0.009	0.758	0.018			6580	-408.9	396.1	15.730	0.005	0.768	0.009	0.371	0.059
5130	104.6	200.1	13.939	0.003	0.624	0.005	0.152	0.020	6598	-445.9	398.6	15.199	0.006	1.125	0.008	0.699	0.059
5131	-260.9	200.4	15.920	0.006	0.651	0.008	0.037	0.045	6619	-395.8	401.5	15.537	0.006	0.806	0.008	0.433	0.042
5135	206.0	201.2	13.889	0.004	1.108	0.010	0.490	0.037	6637	435.9	404.2	15.865	0.006	0.810	0.016	0.344	0.143
5139	160.1	201.6	15.493	0.005	1.055	0.015			6655	-44.4	406.7	15.556	0.006	1.113	0.009	0.660	0.077
5147	163.7	202.4	15.529	0.006	0.713	0.013	-0.283	0.063	6672	518.9	409.4	15.515	0.				

Table 1. Photometric Data in NGC 6716 - Continue

ID	$\Delta\alpha''$	$\Delta\delta''$	V	ϵ_V	B-V	ϵ_{B-V}	U-B	ϵ_{U-B}	ID	$\Delta\alpha''$	$\Delta\delta''$	V	ϵ_V	B-V	ϵ_{B-V}	U-B	ϵ_{U-B}
6828	412.0	432.5	15.797	0.006	1.008	0.016	0.202	0.155	7858	-67.4	567.3	15.830	0.007	1.206	0.011	0.582	0.110
6834	-202.5	432.7	15.932	0.010	0.731	0.012	0.052	0.049	7886	-269.1	571.2	14.748	0.006	1.297	0.008	1.157	0.067
6868	587.4	436.5	15.681	0.005	1.151	0.018	1.038	0.298	7935	-85.9	579.0	14.829	0.004	0.459	0.005	-0.118	0.017
6883	607.4	438.6	12.281	0.003	0.415	0.004	0.224	0.007	7961	-104.6	582.1	15.761	0.006	0.870	0.009	0.742	0.083
6890	137.9	439.7	15.724	0.008	1.417	0.021			7983	153.3	584.4	15.574	0.006	1.080	0.014	0.839	0.198
6891	-148.6	439.7	15.376	0.005	0.851	0.007	0.623	0.066	8015	-203.1	587.8	15.825	0.006	1.214	0.013		
6920	506.7	443.1	15.715	0.005	1.137	0.017			8068	36.5	594.3	15.971	0.006	0.958	0.013		
6946	21.2	446.4	15.955	0.006	1.365	0.011			8069	550.6	594.5	15.787	0.007	1.472	0.024		
6956	388.3	447.0	15.959	0.006	0.723	0.015	0.726	0.189	8076	458.9	595.2	14.841	0.004	1.270	0.011	1.457	0.221
6973	520.3	448.7	15.535	0.005	0.786	0.012	0.138	0.091	8082	421.2	596.0	15.908	0.006	1.613	0.030		
6975	237.8	449.1	15.938	0.006	1.505	0.025			8087	-236.7	596.3	15.490	0.005	0.636	0.007	0.107	0.034
6981	400.4	449.8	15.249	0.005	1.156	0.012	1.254	0.234	8124	277.9	600.5	15.608	0.005	1.220	0.019	1.096	0.292
7018	119.5	454.6	15.768	0.006	0.834	0.013	0.287	0.127	8126	8.5	600.7	12.462	0.006	1.722	0.007		
7036	-253.7	456.7	15.553	0.005	1.363	0.009	1.769	0.199	8135	-44.2	601.3	15.749	0.007	1.116	0.010	1.340	0.165
7061	420.0	458.9	15.931	0.008	0.804	0.017	0.186	0.139	8138	80.5	601.5	15.512	0.006	1.348	0.010		
7098	580.2	463.7	15.991	0.006	0.675	0.015	0.476	0.264	8147	112.7	602.6	15.522	0.009	1.190	0.017	0.822	0.297
7101	586.6	463.9	15.288	0.004	0.636	0.009	0.098	0.093	8148	-22.1	602.8	14.786	0.006	1.733	0.009		
7126	-367.3	467.4	15.266	0.005	1.572	0.009	1.893	0.196	8154	-139.7	603.5	14.180	0.003	1.098	0.005	0.890	0.034
7135	355.4	468.6	14.263	0.003	0.706	0.006	0.308	0.028	8166	606.6	605.3	13.832	0.006	0.576	0.008	0.019	0.019
7170	330.7	473.1	14.857	0.003	0.630	0.008	0.356	0.178	8171	-379.8	605.7	13.816	0.002	0.524	0.004	0.013	0.009
7186	-466.6	474.6	13.873	0.002	1.228	0.004	1.122	0.028	8173	-64.5	606.0	15.855	0.007	0.656	0.009	0.085	0.048
7192	28.3	476.1	15.591	0.005	1.270	0.008			8186	-306.8	607.9	14.717	0.005	0.511	0.006	-0.038	0.014
7202	-186.4	477.2	15.715	0.006	0.396	0.007	0.371	0.038	8197	436.5	609.3	15.404	0.005	1.180	0.014	1.326	0.309
7225	582.5	480.0	15.578	0.010	1.211	0.020			8198	393.1	609.3	12.425	0.003	0.391	0.004	0.261	0.008
7245	5.7	483.0	15.750	0.005	0.735	0.008			8208	-339.4	610.0	15.664	0.007	1.123	0.011		
7267	-52.5	485.3	15.762	0.008	0.832	0.010	0.369	0.060	8209	560.5	610.1	15.303	0.006	1.180	0.014	0.875	0.179
7287	71.1	487.4	15.615	0.005	1.180	0.009			8211	-163.1	610.2	15.929	0.008	1.437	0.014		
7291	308.4	488.0	15.246	0.004	1.283	0.014	1.231	0.234	8213	167.4	610.5	15.209	0.006	0.686	0.010	0.177	0.062
7315	-242.3	490.0	15.809	0.006	1.175	0.010	1.297	0.153	8216	-196.8	611.4	15.713	0.006	1.193	0.010	0.775	0.120
7316	-49.5	490.1	15.791	0.008	1.134	0.012	1.001	0.138	8219	261.0	611.7	15.579	0.005	1.087	0.014	0.518	0.158
7324	-330.0	491.1	13.693	0.003	1.791	0.004	2.183	0.076	8230	464.4	612.9	15.533	0.005	1.396	0.019		
7355	551.5	495.6	13.095	0.002	0.302	0.003	0.402	0.040	8238	544.0	614.4	15.713	0.007	1.092	0.017	0.925	0.229
7356	418.8	495.7	15.022	0.004	0.437	0.007	0.154	0.041	8256	-92.0	616.7	15.179	0.005	1.262	0.007	1.326	0.111
7362	-31.5	496.5	15.249	0.008	1.138	0.012	0.735	0.067	8258	57.3	617.1	15.745	0.006	0.631	0.010	0.021	0.088
7375	607.2	498.4	15.672	0.005	0.666	0.012	0.047	0.077	8262	-435.8	617.7	15.070	0.005	1.140	0.008	0.963	0.068
7386	-311.4	499.4	14.229	0.003	1.182	0.005	0.914	0.027	8268	-344.7	618.1	14.408	0.004	1.460	0.006	1.454	0.079
7400	-167.7	501.7	15.540	0.004	1.082	0.006	0.968	0.087	8272	332.2	618.8	12.256	0.003	1.664	0.005	2.079	0.050
7473	91.0	509.8	15.901	0.008	0.736	0.019	-0.051	0.301	8280	425.2	619.7	13.919	0.003	0.526	0.004	-0.028	0.017
7500	422.8	512.1	15.487	0.005	1.488	0.020			8282	241.4	620.2	15.992	0.007	0.696	0.017	0.814	0.203
7503	70.5	512.3	15.834	0.005	0.760	0.008	0.090	0.108	8294	-21.4	621.3	13.172	0.008	1.265	0.009	1.030	0.019
7523	-185.3	515.4	15.967	0.006	1.163	0.010	0.951	0.157	8296	614.5	621.5	9.851	0.028	0.396	0.029	0.220	0.007
7525	424.5	515.7	15.131	0.004	1.420	0.015			8311	-0.4	624.1	15.573	0.006	1.160	0.010		
7532	598.2	517.1	15.802	0.010	1.066	0.021			8314	250.0	624.2	13.450	0.004	1.141	0.006	1.002	0.041
7549	366.1	519.3	15.070	0.004	1.295	0.013	0.879	0.160	8318	-369.2	624.6	15.457	0.005	1.301	0.009	1.741	0.223
7558	613.8	521.2	10.952	0.009	0.070	0.010	0.174	0.008	8328	392.1	625.8	10.650	0.004	1.239	0.005	1.522	0.008
7559	-163.0	521.2	15.596	0.007	1.015	0.011	0.528	0.092	8331	20.5	625.9	15.779	0.006	0.923	0.010		
7579	535.8	525.0	13.033	0.003	0.465	0.004	0.193	0.016	8334	454.0	626.2	15.988	0.006	1.150	0.021		
7602	25.0	529.3	15.461	0.005	0.596	0.007	0.162	0.074	8336	-213.8	626.5	15.098	0.005	0.638	0.006	0.008	0.025
7637	588.5	535.4	15.838	0.006	0.989	0.016			8337	411.9	626.6	14.436	0.004	0.962	0.008	0.448	0.056
7647	-151.8	536.7	11.499	0.009	0.716	0.010	0.380	0.035	8338	187.8	626.7	14.859	0.005	0.803	0.009	0.377	0.066
7659	496.6	538.5	14.447	0.003	1.433	0.009	0.971	0.125	8343	-287.5	627.1	15.548	0.005	1.468	0.009	0.922	0.140
7667	269.7	539.7	15.952	0.006	1.072	0.020	0.618	0.222	8344	46.0	627.2	15.709	0.006	0.858	0.009		
7680	554.3	542.3	13.207	0.003	1.190	0.005	1.140	0.034	8355	-8.3	628.9	14.591	0.006	0.736	0.007	0.120	0.018
7684	-313.0	542.9	15.078	0.004	0.766	0.006	0.120	0.022	8356	244.8	629.1	14.763	0.004	1.259	0.011	1.352	0.171
7687	417.7	543.4	13.910	0.002	1.205	0.005	1.157	0.066	8377	252.1	631.7	15.042	0.006	0.842	0.011	0.369	0.081
7688	441.6	543.5	13.452	0.002	0.570	0.004	0.164	0.013	8380	402.6	632.0	15.628	0.026	1.067	0.053		
7693	-275.8	544.9	15.392	0.005	0.660	0.007	0.163	0.029	8410	-475.4	637.8	14.624	0.005	1.124	0.006	0.773	0.040
7705	92.2	546.2	14.757	0.005	1.415	0.010			8419	156.8	638.6	15.985	0.009	0.762	0.018	-0.057	0.129
7706	26.6	546.2	15.479	0.005	1.247	0.010	1.312	0.347	8436	337.4	640.9	13.346	0.004	1.312	0.006	1.282	0.053
7722	-228.7	548.2	15.534	0.005	1.373	0.009	1.512	0.186	8438	-35.9	641.0	10.758	0.004	0.121	0.00		

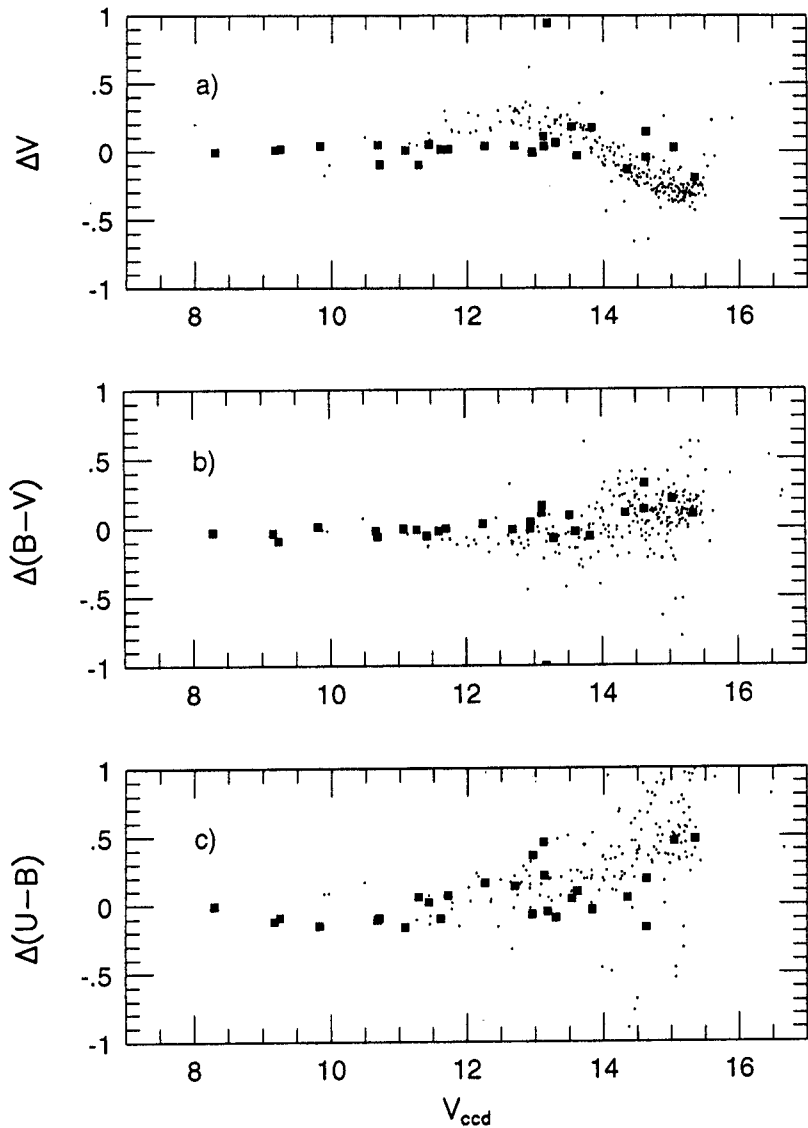


Fig. 3. Comparisons of our ccd data with the photometric data of Grice & Dawson (1990). $\Delta = (\text{this obs} - \text{GD})$. Filled rectangles denote the photoelectric data and small dots denote the photographic data. A star (no. 18), which has $\Delta V \simeq 0.^m 95$, $\Delta(B - V) \simeq -1.^m 00$, is excluded in the $\Delta(B - V)$ diagram. There are some systematic deviations for stars fainter than 13 mag in GD's photographic data.

a single photometric error. The resulting photometric data for stars brighter than 16^m are given in Table 1.* To determine the relative coordinate of each star from no. 1 star, the tilted angle and the plate scale of the CCD frame are corrected using the stars in the Hubble Guide Star Catalog. The resulting photometric errors in magnitude and colors are shown in Fig. 2. The monotonic increase of errors with increasing V magnitude can be seen in Fig. 2. The errors of $(U - B)$ color are larger than those of V magnitude and $(B - V)$ color index because of the lower quantum efficiency of the CCD chip at the short wavelength region and the limited exposure time by a tracking accuracy of the telescope.

As seen in Fig. 3, there is no systematic differences between GD's photoelectric data and our CCD data except only one star (no. 18), which has $\Delta V \approx 1^m$. This one is out of boundary in $\Delta(B - V)$ diagram. This large differences for the star seem to be arisen from the uncertainty of GD's photoelectric data because the LD's photographic data of the star are consistent with our CCD data. On the other hand, comparison with the GD's photographic data shows

* Please contact the author(MYC) through the network to get the whole data.

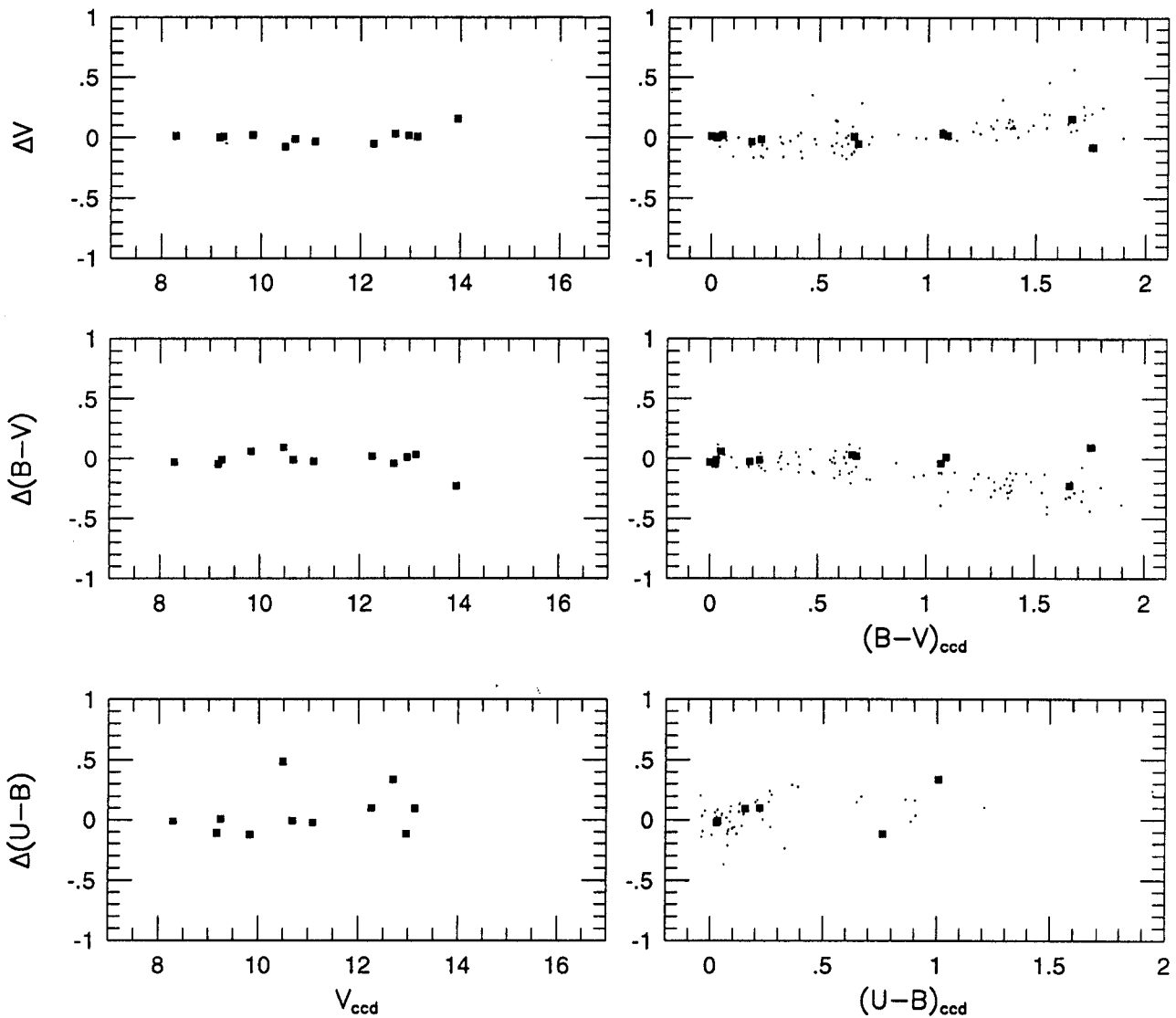


Fig. 4. Comparisons of our photometric data with the photometric data of Lindoff(1971). $\Delta = (\text{this obs} - \text{LD})$. Filled rectangles denote the photoelectric data and small dots denote the photographic data. No systematic difference appears in the left panels, comparisons along V mag. In right panels, there are weak systematic differences in $(B - V)$ between our CCD data and LD's photographic data along $(B - V)$ index.

very large systematic errors in the magnitude and the colors for the stars fainter than $V \approx 13$. This is certainly due to observational uncertainty in the GD's data of the faint stars. We also compared our data with the LD's data in Fig. 4. There seems to be no systematic magnitude difference between our CCD data and LD's photoelectric data along V mag. But in the right panels of Fig. 4, a weak systematic effect on color is seen in the sense that the LD's photoelectric color is redder with increasing $(B - V)_{\text{ccd}}$ than our CCD color. As GD argued already, the possible cause of this systematic differences is likely to be the small number of photoelectric stars.

III. THE COLOR-MAGNITUDE DIAGRAM

(a) The Determination of the Fundamental Parameters of the Cluster

The resulting $(B - V)$ - V diagram(CMD), $(B - V)$ - $(U - B)$ diagram(C-C diagram) of the stars in NGC 6716 are

NGC 6716

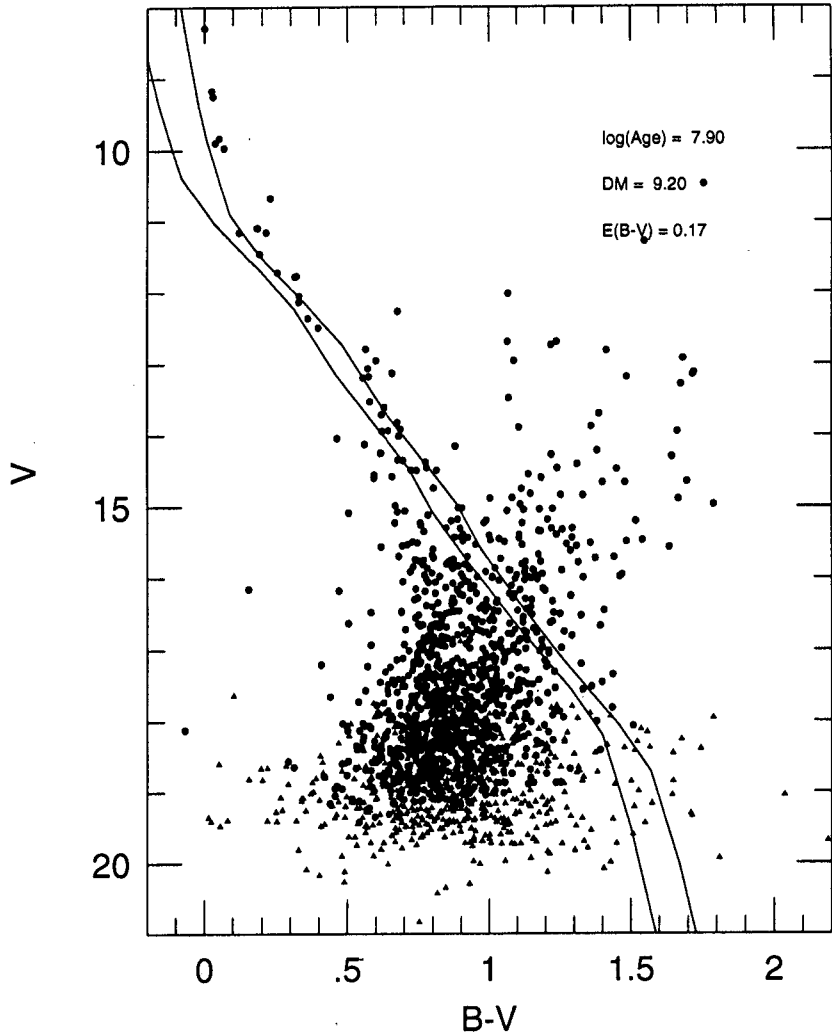


Fig. 5. CMD for all the stars(7827) studied in the region of NGC 6716. Small filled triangles denote the stars of which photometric errors are larger than 0.1 mag. The fiducial ZAMS is drawn adopting $E_{B-V} = 0.17$ & $(V - M_V) = 9.7$.

shown in Figures 5 and 6, where the small triangles present the stars of photometric error larger than 0.1 magnitude and the solid line represents ZAMS line(Lee & Sung 1995). The number of stars plotted in Fig. 5 is 7827. Among these stars, the cluster members seem to be very small as shown by sparse bright main sequence stars down to $V \approx 15$. The blue main-sequence and lack of giant stars in Fig. 5 imply that NGC 6716 is not so old. Along the main sequence, there appear two distinct gaps at $V \approx 10.5$ and 13. The turnoff(TO) point of main-sequence is located at $V \approx 8.9 \pm 0.3$ and $(B - V) \approx 0.01 \pm 0.01$. At the fainter part of the CMD, we can see some features different from the cluster sequence. There are the Galactic nuclear bulge components which will be discussed in the next section.

Low signal to noise ratio of the U frames makes the number of stars reduced and a large dispersion at the color of $0.5 < (B - V) < 1.0$ in the C-C diagram(Fig. 6). The red stars ($(B - V) > 1.1$) are located below the ZAMS line, because they are not the main-sequence stars but the giant stars. It is confirmed by their right-upper locations in the CMD.

To minimize the effects by the contamination of field stars and Galactic nuclear bulge components in the determination of color excess and distance modulus of NGC 6716, only bright stars with small photometric errors in

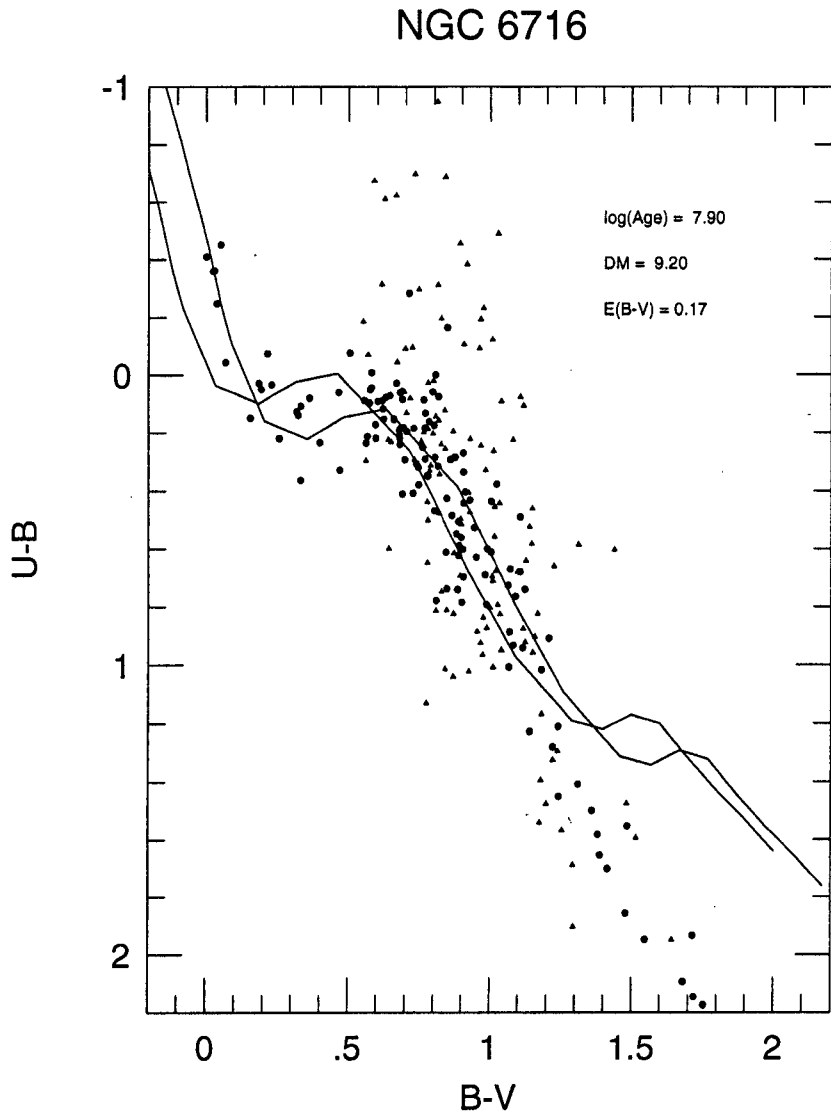


Fig. 6. Color-color diagram of NGC 6716. Low S/N ratio of U frame makes the number of stars reduced in this diagram. Fiducial ZAMS and color excess corrected ZAMS are plotted. Symbols in this diagram mean the same as in Fig. 5.

$(U - B)$ index ($V < 15$, $\epsilon(U - B) < 0.1$) and stars within 5 arcmin from the cluster center are selected. We present a new C-C diagram of NGC 6716 in Fig. 7. Applying the fiducial ZAMS line to this diagram, the color excess of $E(B - V) = 0.18$ is estimated. The three member stars in Table 2 were measured by LD with slit spectrograph. We derived their color excess from their spectral type and intrinsic color, which are given in Table 2. The mean value of $E(B - V)$ from Table 2 is about 0.14. From the above two estimates of color excess, we adopted 0.17 ± 0.03 for the color excess of NGC 6716. The error in the distance modulus induced by the estimated error in color excess is about 0.1 magnitude.

The ZAMS of Lee & Sung(1995) was fitted to CMD for stars with V magnitude in the $13^m \sim 15^m$ in the central region because the stars brighter than 13^m are leaving ZAMS. The apparent distance modulus of the cluster ($V - M_V$) is 9.7 ± 0.15 mag for $R=3.0$. This distance modulus is a little bit larger than previous results such as 9.2 mag(LD) and 8.9 mag(GD).

An isochrone of $\log t = 7.9$ (Schaller *et al.* 1992) are taken to fit the sequence of bright main sequence stars in Fig. 8. The two sequences(dashed line) which correspond to a half and twice cluster age are plotted also only for a comparison.

NGC 6716

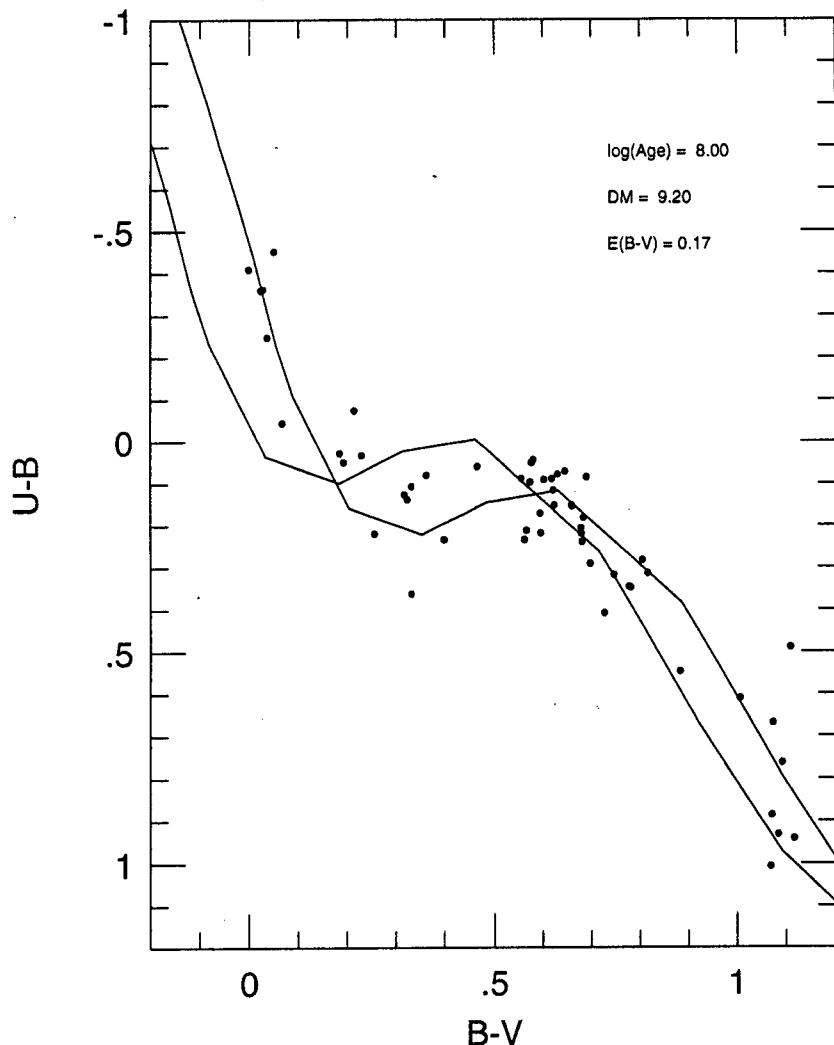


Fig. 7. Cleaned color-color diagram. The selected stars are located within 5 arcmin from the center of the cluster and its photometric errors of ($U - B$) index is less than 0.1 mag. Estimated color excess from this color-color diagram is 0.17 mag.

Table 2. Color Excess of Stars with Known Spectral Types

ID	V	This OBS $B - V$	$U - B$	Sp^a	$(B - V)_{sp}^b$	$E(B - V)_{sp}$
3	9.170	0.024	-0.360	B8V	-0.11	0.134
46	8.293	0.000	-0.410	B7IV	-0.13	0.130
55	9.248	0.029	-0.362	B8IV	-0.11	0.139

^a From Lindoff(1971)

^b $(B - V)_{sp}$ values of given spectral type is adopted from Lee(1985)

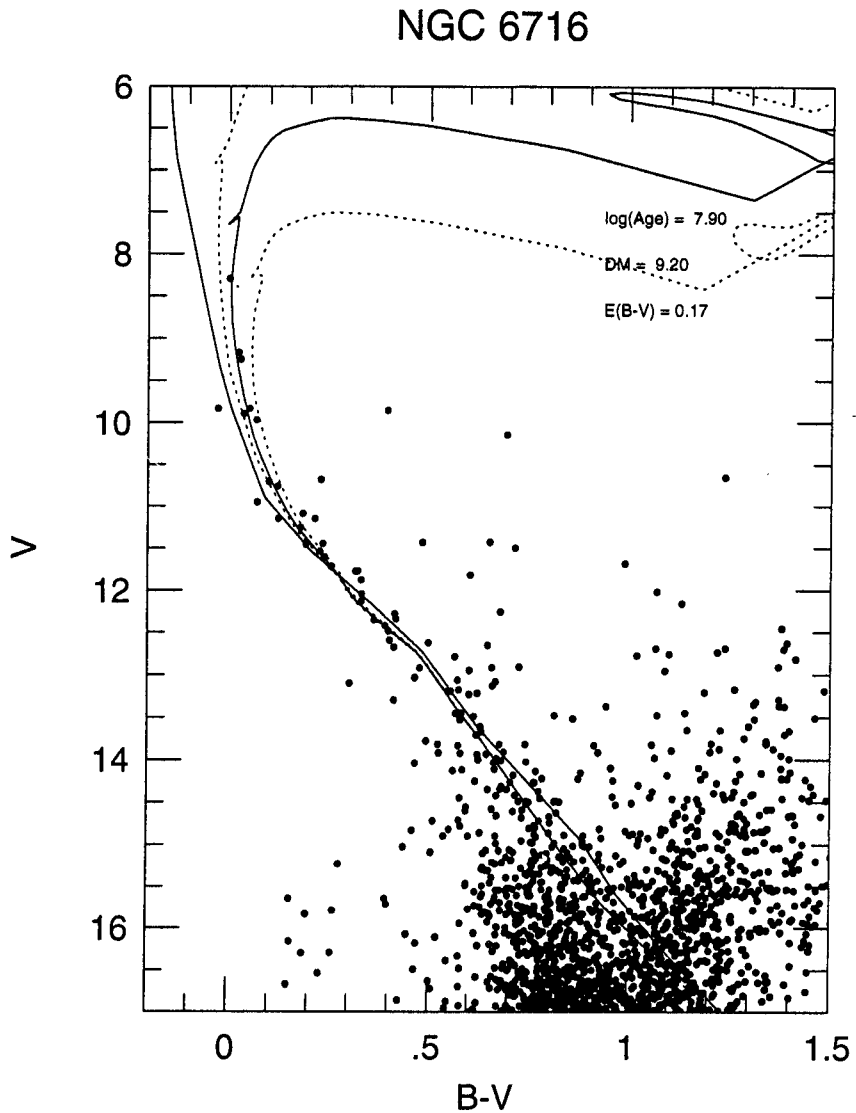


Fig. 8. CMD of NGC 6716 with isochrones. The isochrone is from Schaller *et al.* (1992), for $Z=0.02$ and $\log t = 7.9$ (solid). Two additional isochrones for $\log t = 7.6$ & 8.2 (dotted) are plotted only for comparison. ZAMS(thick solid) are adopted from Lee & Sung(1995).

We can also estimate the age of cluster by using the relation between age and $(B - V)_{bt}$ color index of the main-sequence turn-off (Meynet *et al.* 1993) :

$$\log t = -14.368(B - V)_{bt}^2 + 1.861(B - V)_{bt} + 8.589, \quad (2)$$

The above relation is valid only for the ranges of $6.6 < \log t < 9.6$ and $-0.18 < (B - V)_{bt} < 0.00$. As we already estimated, the TO color index of NGC 6716 is $(B - V) = 0.012 \pm 0.01$, and the extinction free index is $(B - V)_{bt} = -0.158 \pm 0.03$. Then, the above relation yields $\log t = 7.94 \pm 0.2$, which is exactly consistent with the isochrone age. The uncertainty in age estimate comes mostly from the errors involved in color excess estimation. Therefore it is very important to determine the color excess as accurate as possible.

(b) The Components of Galactic Nuclear Bulge

The nuclear bulge of the Galaxy is the nearest example of an old, metal-rich stellar population, which is seen in

elliptical galaxies and in the bulges of other spiral galaxies. The spectroscopic observation of the K type giants in "Baade's Window" at $l = 1^\circ$, $b = 3.9^\circ$ (Baade 1963) has confirmed the metal-rich nature of the bulge stars(Whitford & Rich 1983; Rich 1988). Recent investigations have concerned on the M type giants in the bulge, which also have a high metal content, as including these high metal M giants rather than their solar neighborhood counterparts in galaxy models significantly improves the match of the observed infrared colors of E and SO type galaxies(Frogel & Whitford 1987). Readers may note Frogel(1988) for an extensive review on bulge research.

The distinctive features of the observed bulge components, compared with Terndrup(1988)'s CMD, in CMD can be summarized as follows:

- (1) Turn-off of the main-sequence of the galactic bulge is not clear
- (2) An extended, mild sloped red giant branch is shown, but no clump appears.
- (3) A blue sequence, which gradually becomes redder at faint magnitudes and crosses the bulge sequence near the upper end of the turn-off, is shown. These are expected as the main-sequence stars between the cluster and the galactic bulge.

The bulge components and field main-sequence stars restricted our investigations to bright stars and so the luminosity function and mass function of the cluster are also meaningful only for bright stars. As the bulge components are dominant at faint region ($V > 15^m$), it is meaningless statistically to subtract the bulge components and field stars from the CMD by using Terndrup's data or galaxy model.

IV. LUMINOSITY FUNCTION AND MASS FUNCTION

To derive a luminosity function of NGC 6716, it is necessary to have a complete data of member stars brighter than a certain limiting magnitude, excluding field stars in the cluster field. As mentioned in the previous section, we set $V_{lim} = 14.5$ since the bulge components and field stars are dominant at $V > 15^m$. We believe that a nearly complete set of stars with $V < 14.5^m$ is available because V_{lim} is far from the frame limit magnitude $V \approx 19.5^m$ and PSF fitting photometry (DAOPHOT) can measure a magnitude of each star from crowded stars quite well.

Since there is no proper motion study for this cluster, the member stars are selected considering the locations in the CMD and C-C diagram. Their spatial distribution is shown in Fig. 9, where most of the stars are located within 6.5 arcmin from the center of the cluster. There are some stars in SE & NW directions along the galactic plane.

Table 3. The Luminosity Function of NGC 6716

M_V	V	N_{tot}	N_{field}	N_{Member}
-1.7	8.0	1	0	1
-0.7	9.0	2	0	2
+0.3	10.0	7	4	3
+1.3	11.0	15	6	9
+2.3	12.0	23	21	12
+3.3	13.0	52	38	14
+4.3	14.0	123	89	34
sum		223	148	75

The luminosity functions for the field stars and the member stars are given in Table 3 and the luminosity function for the member stars is shown in Fig. 10, where the error bars marked on the figure denote simple statistical errors. An overall feature of the luminosity function shows roughly a monotonic function with M_V , having small jumps at $M_V = +1.3$, and $+4.3$ bins. The sudden increase at $M_V = +4.3$ seems to be arisen from an under-correction for field stars.

The initial mass function of a cluster is of more fundamental importance than the luminosity function, since the latter contains the effects of stellar evolution, dynamical evolution, and mass-luminosity relation. To derive mass of each star, we used the stellar mass distribution along isochrone. The mass function, $\xi(\log m)$ is defined as a number

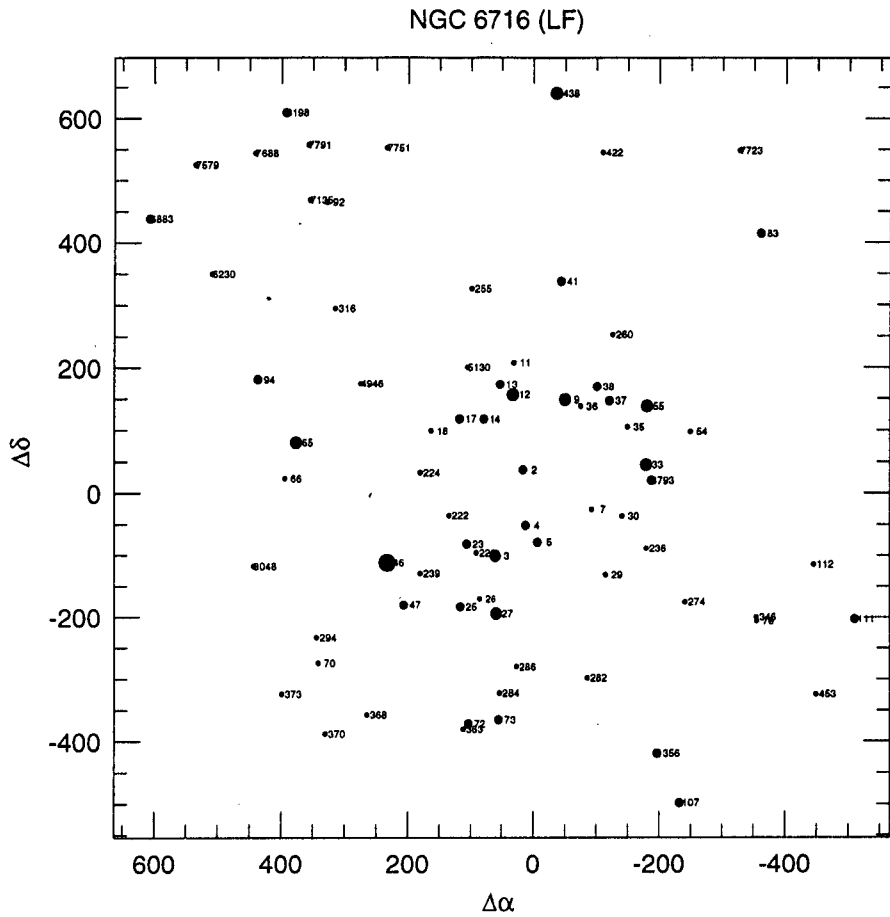


Fig. 9. Spatial distribution of stars which are used to derive luminosity function of NGC 6716. Most stars are located within $r < 6.4$ arcmin.

of stars per unit logarithmic mass and its gradient Γ is defined as

$$\Gamma \equiv \frac{d \log(\xi(\log(m)))}{d \log(m)}. \quad (3)$$

Table 4. The Mass Function of NGC 6716

$\log m$	N	$\log(\xi(\log m))$
0.65	3	0.477
0.55	3	0.477
0.45	3	0.477
0.35	6	0.778
0.25	9	0.954
0.15	14	1.146
0.05	35	1.544
sum	75	

NGC 6716 (LF)

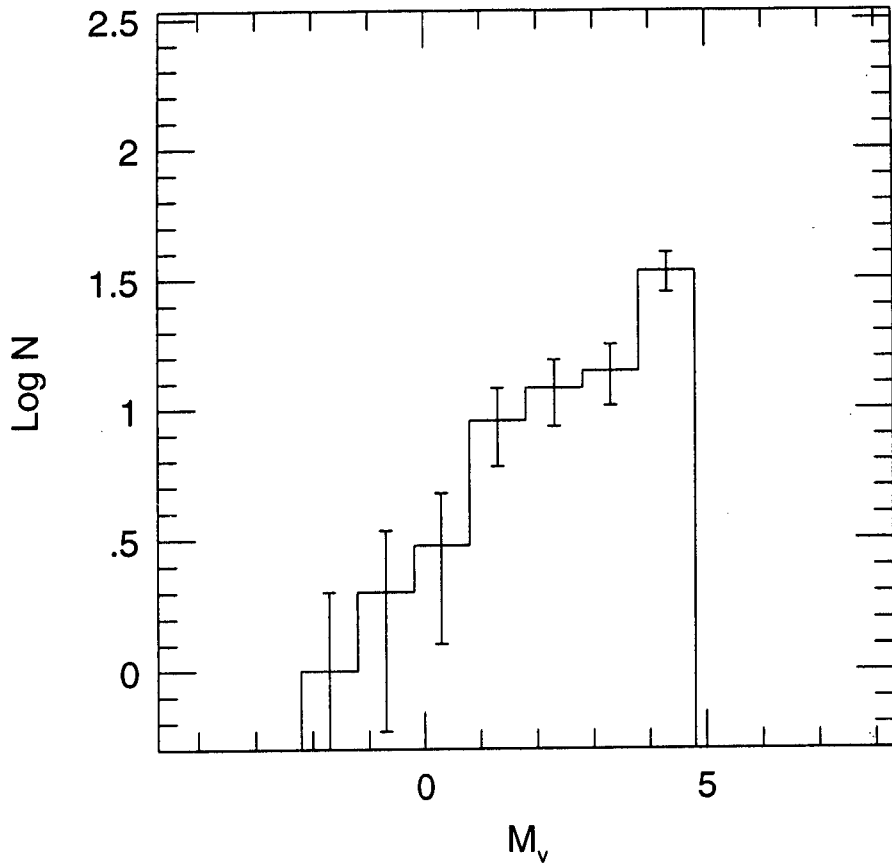


Fig. 10. The luminosity function of NGC 6716. It is limited by the galactic bulge components down to ~ 14.5 mag. The error bars are simple statistical uncertainties.

So, the number of stars counted in equal interval of $\Delta \log m = 0.1$ are given in Table 4 and in Fig. 11, where the bars denote statistical errors. The gradient of the derived mass function is obtained as $\Gamma = -1.85 \pm 0.05$ by the weighted linear regression algorithm. The number of stars in a bin were used as weights. In the regression, the first bin and the final bin were excluded because they are not filled. We believe that the gradient is meaningful within the boundary defined by statistical error, because the final bin was excluded which may include the bulge components. The data points of low mass bin ($\log m = 0.35, 0.25, 0.15$) are located on the line. There is a small jump at $\log m = 0.35$, which is related to the small jump in the luminosity function at $M_V = 1.3$. But it seems to be not definite due to small number.

V. SUMMARY AND DISCUSSION

This paper has been devoted to the presentation of a new color-magnitude diagram and color-color diagram for the intermediate age open cluster NGC 6716 which has been studied by Lindoff(1971) and Grice & Dawson(1990). The new CMD supersedes the previous ones for the larger number of objects detected and for the extension of the MS. This fact allows us to better estimate the fundamental parameters of the cluster, such as the color excess, the distance modulus and the age. Adopting the fiducial ZAMS from Lee & Sung (1995), we obtained a color excess $E_{B-V} = 0.17 \pm 0.03$, a distance from the sun 690pc ($(V - M_V)_0 = 9.2 \pm 0.1$). This color excess is close to the values given by Lindoff(1971) and Grice & Dawson(1990), but the distance modulus is a little bit larger than previous ones. The comparisons of the observed CMD with theoretical isochrones from Schaller *et al.* (1992) show a good

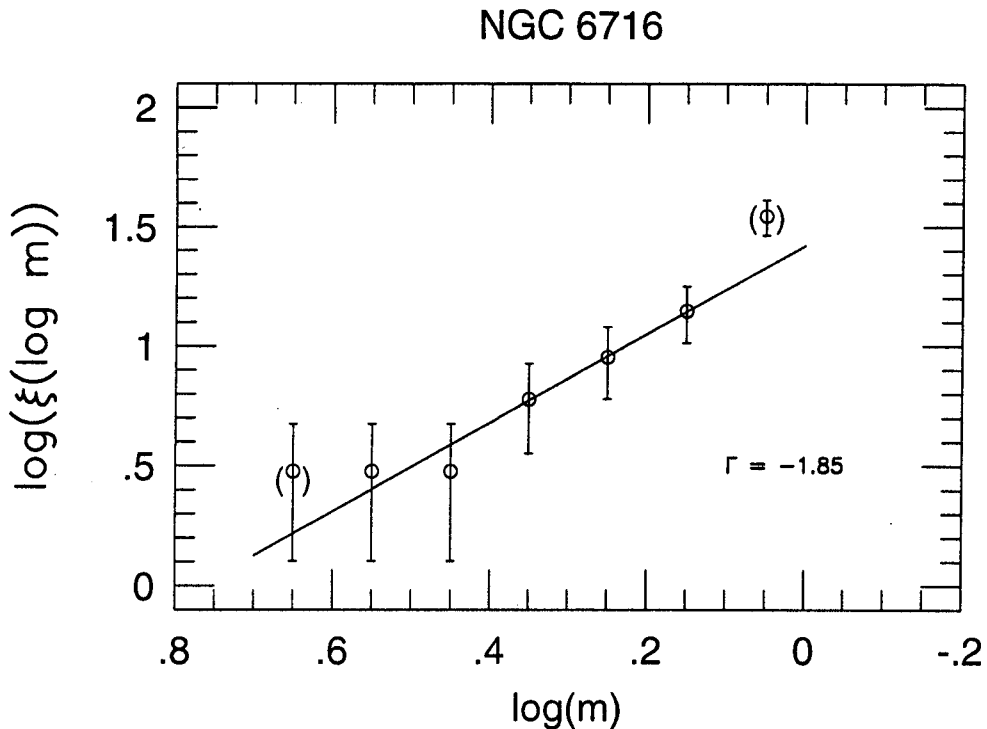


Fig. 11. Mass Function of NGC 6716. The bins marked as () were excluded to determine the gradient of Mass function ($\Gamma = -1.85$).

agreement with isochrone for $\log t = 7.9$ (8×10^7 years).

In the CMD for stars fainter than 15 mag, the galactic bulge components are dominant and their distribution shows a similar feature in the CMD shown in Terndrup(1988) at $l = 0^\circ, b = -10^\circ$ region.

We derived the luminosity function and the mass function of the cluster by using bright member stars. The estimated gradient of mass function is $\Gamma = -1.85 \pm 0.05$, which is steeper than that for the solar neighborhood field stars(Salpeter 1955), $\Gamma = -1.35$. There is no bump and dip in the Mass Function.

ACKNOWLEDGEMENT

This research was supported by MOST's(Ministry of Science and Technology) Research Fund through KAO. We thank Prof. K.C. Freeman for his generous allotments of observing time with the SSO's 1m telescope, and staffs of SSO for their help & guiding during observation period. One of us (MYC) is grateful to Mr. Y.-J. Moon for his careful reading and to Mr. B.-G. Park and Dr. S.-L. Kim for his assistance in preparation of drawings.

REFERENCES

- Baade W. 1963, in *Evolution of Stars and Galaxies*, edited by C.P. Gaposkin (Harvard University, Cambridge), p.279.
- Bessell, M.S. 1990, PASP, 102, 1181.
- Frogel J.A. 1988, ARAAp, 26, 51.
- Frogel J.A., Whitford A.E. 1987, APJ, 320, 199.
- Graham, J. A. 1981, PASP, 93, 29.
- Grice N.A., Dawson D.W. 1990, AJ, 102, 881(GD).
- Landolt, A. U. 1992, AJ, 104, 340.
- Lee S.-W. 1985, *Astronomical Observation and Analysis*, (1st Edition Seoul:MinEum Publishing Co.)
- Lee S.-W., Sung W. 1995, JKAS, 28, 45.

- Lindoff U. 1971, A&A, 15, 439(LD).
- Meynet G., Mermilliod J.-C., Maeder A. 1993, A&AS, 98, 477.
- Rich R.M. 1988, AJ, 95, 828.
- Ruprecht J. 1966, *Bull. Astr. Inst. Czechoslovakia*, 17, 34.
- Salpeter E.E. 1955, ApJ, 121, 161.
- Schaller, G., Schaerer, D., Meynet, G., Maeder, A. 1992, A&AS, 96, 269.
- Stetson, P.B. 1987, PASP, 99, 191.
- Stetson P.B. 1991, in *The Formation and Evolution of Star Clusters*, edited by K. Janes (ASP conference Series Vol 13), p.88.
- Terndrup D.M. 1988, AJ, 96, 884.
- Trumpler R.D. 1930, *Lick Obs. Bull.*, 14, 174.
- Turner D.G., Pedreros M. 1985, AJ, 90, 1231.
- Whitford A.E., Rich R.M. 1983, APJ, 265, 748.